

AD-A249 260

COPY FOR REPRODUCTION PURPOSES

REP

Form Approved  
OMB No. 0704-0188

2

Public reporting burden for this gathering and maintaining the collection of information, including the review of existing data sources, gathering and maintaining the data needed, and completing and reviewing the collection of information, send comments regarding this burden estimate or any other aspect of this collection of information, including suggestions for reducing this burden, to Washington Headquarters Services, Directorate for Information Operations and Reports, 1215 Jefferson Davis Highway, Suite 1204, Arlington, VA 22202-4302, and to the Office of Management and Budget, Paperwork Reduction Project (0704-0188), Washington, DC 20503.

including the time for reviewing instructions, searching existing data sources, gathering and maintaining the data needed, and completing and reviewing the collection of information, send comments regarding this burden estimate or any other aspect of this collection of information, including suggestions for reducing this burden, to Washington Headquarters Services, Directorate for Information Operations and Reports, 1215 Jefferson Davis Highway, Suite 1204, Arlington, VA 22202-4302, and to the Office of Management and Budget, Paperwork Reduction Project (0704-0188), Washington, DC 20503.

1. AGENCY USE ONLY (Leave blank)		2. REPORT DATE		3. REPORT TYPE AND DATES COVERED 7/1/91-12/31/91	
4. TITLE AND SUBTITLE Scattering Mechanisms for Semiconductor Transport Calculations, Chapt. in Monte Carlo Device Simulation: Full Band and Beyond, pp. 27-66				5. FUNDING NUMBERS DFAA03-89-K-0037	
6. AUTHOR(S) Jeff Bude Edited by Karl Hess				DTIC ELECTE APR 30 1992 S C D	
7. PERFORMING ORGANIZATION NAME(S) AND ADDRESS(ES) Beckman Institute and Coordinated Science Laboratory University of Illinois Urbana, IL 61801					
8. PERFORMING ORGANIZATION REPORT NUMBER				10. SPONSORING/MONITORING AGENCY REPORT NUMBER ARO 26711.17-EC	
9. SPONSORING/MONITORING AGENCY NAME(S) AND ADDRESS(ES) U. S. Army Research Office P. O. Box 12211 Research Triangle Park, NC 27709-2211				11. SUPPLEMENTARY NOTES The view, opinions and/or findings contained in this report are those of the author(s) and should not be construed as an official Department of the Army position, policy, or decision, unless so designated by other documentation.	
12a. DISTRIBUTION / AVAILABILITY STATEMENT Approved for public release; distribution unlimited.				12b. DISTRIBUTION CODE	
13. ABSTRACT (Maximum 200 words) We have applied our Monte Carlo approach to impact ionization to various important semiconductor materials including GaAs, InP and InAs. We find that in all these materials the ionization mechanism is quantitatively different to what has been described in previous simplified models, such as Shockley's lucky electron theory. With regard to quantum transport, we have continued our work on the electron-electron interaction in simple nanostructures. The main goal of this study is to investigate whether Coulomb blockade effects continue to exist at the molecular level when quantization effects become significant.					
14. SUBJECT TERMS Electronic Transportation and Semiconductor Heterostructures				15. NUMBER OF PAGES	
				16. PRICE CODE	
17. SECURITY CLASSIFICATION OF REPORT UNCLASSIFIED		18. SECURITY CLASSIFICATION OF THIS PAGE UNCLASSIFIED		19. SECURITY CLASSIFICATION OF ABSTRACT UNCLASSIFIED	
				20. LIMITATION OF ABSTRACT UL	

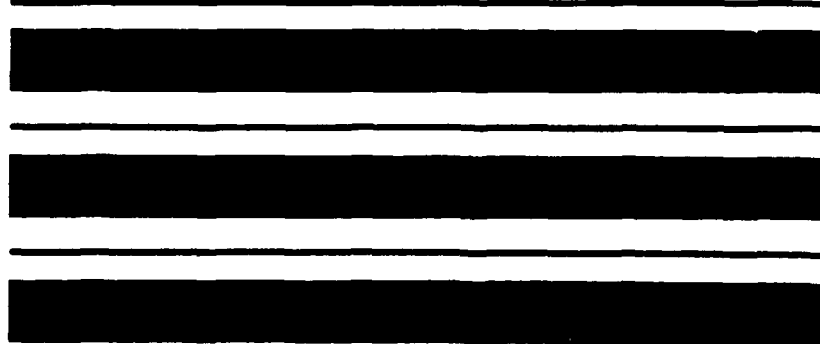
---

# Monte Carlo Device Simulation: Full Band and Beyond

---

edited by

**Karl Hess**



---

**Kluwer Academic Publishers**

**92 4 28 069**

Accession For	
NTIS ORNL	<input checked="" type="checkbox"/>
DTIC TAB	<input type="checkbox"/>
Unannounced	<input type="checkbox"/>
Justification	
By _____	
Distribution/	
Availability Codes	
Dist	Avail and/or Special
A-1	



**92-11526**

# SCATTERING MECHANISMS FOR SEMICONDUCTOR TRANSPORT CALCULATIONS

J. Bude

*Beckman Institute for Advanced Science and Technology and ECE  
University of Illinois at Urbana-Champaign, Illinois 61801*

Monte Carlo simulations for transport in semiconductors numerically solve the Boltzmann equation while offering the physically intuitive picture of free flights and carrier scatterings on a microscopic level. The aim of a good Monte Carlo simulator is to give the most physically correct realisation of the scattering and free flight processes in an efficient manner. This chapter treats the scattering mechanisms and their implementation in detail. The basic scattering mechanisms treated in this chapter fall into the categories of phonons, static impurities, and scattering due to the coulomb potential of other carriers (carrier-carrier interactions). Photon scattering is important in specific cases (radiative recombination rates for instance), but occurs on time scales much longer than the scattering processes mentioned above, and so is not usually a factor in determining basic transport parameters.

In almost all approaches to electron transport in crystals, the electrons are decoupled from the ions, impurities, and from each other, and familiar Bloch states are assumed for a complete basis set for the electrons. Then, the effect of each of these interactions is reintroduced as a perturbation to the simple, one-electron states forcing transitions between them, i.e. scattering. In order to accomplish the decoupling, one makes use of the adiabatic approximation (Born-Oppenheimer approximation) which is the topic of the first section. However, the Boltzmann equation, which is the basis for all Monte Carlo simulations, is a fully classical equation, originally derived for transport of gasses whose constituents interact weakly. The generalisation of this equation to the semiclassical regime in which collisions are seen as localised events in space and time but calculated quantum mechanically is a simple extension of the classical Boltzmann equation. The steps leading to this extension which are relevant to the treatment of scattering are discussed in the second section of this chapter. It is then easy to obtain the proper form for the scattering rates. Then, a short discussion of dielectric screening (an important consideration for the calculation of scattering) is given. The remainder of the chapter is devoted to the calculation of specific scattering rates and their implementation in Monte Carlo simulations.

# 1 The Adiabatic Approximation

To begin our discussion of electron transport in semiconductors, we define electrons to be in one of three classes: *core electrons*, which are tightly bound to the nuclei, *valence electrons*, which are loosely bound and form the covalent bonds between ions, and *conduction electrons*. Valence electron states lie beneath the band gap and are completely filled at zero temperature. Electrons which occupy the excited states above the band gap are termed conduction electrons. In the following discussion of the adiabatic approximation, the crystal is decomposed into *ions* (the nuclei and the core electrons treated as a unit moving rigidly together) and the *outer electrons* which are either valence electrons or conduction electrons.

The effect of the lattice (ions) on electron transport is typically evaluated by making use of the *adiabatic approximation* which separates the electronic (outer electrons) and ionic motion so that their interaction may be treated in perturbation theory. The crystal Hamiltonian in the adiabatic approximation can be derived from the general Hamiltonian as follows. The full Hamiltonian is [1],

$$H_{tot} = T_{ion}(\{R\}) + U_{ion}(\{R\}) + T_{el}(\{r\}) + U_{ee}(\{r\}) + U_{ei}(\{r\}, \{R\}) \quad (1)$$

where the ionic and electronic kinetic energies are  $T_{ion}$  and  $T_{el}$ , and the potential energies  $U_{ion}$  and  $U_{ee}$ . ( $U_{ee}$  is the electron-electron interaction.)  $U_{ei}$  is the electron-ion interaction, and the ion and electron coordinates are denoted by  $\{R\}$  and  $\{r\}$ . Because the ions are more massive than the electrons, they will move much more slowly. The key step in formulating the adiabatic approximation is the assumption that the electrons respond *adiabatically* to the motion of the ions — the ion motion does not force transitions between electronic states, but the electron eigen-states evolve adiabatically as the ion positions change. Then, for a fixed set of ion coordinates  $\{R\}$ , there corresponds a full set of electronic eigen-functions:

$$[T_{el}(\{r\}) + U_{ee}(\{r\})] \psi_n(\{r\}, \{R\}) = E_n(\{R\}) \psi_n(\{r\}, \{R\}), \quad (2)$$

$$+ U_{ei}(\{r\}, \{R\}) \psi_n(\{r\}, \{R\}) = E_n(\{R\}) \psi_n(\{r\}, \{R\}), \quad (3)$$

and the eigen-function of the full Hamiltonian  $H_{tot} \Phi = E_{tot} \Phi$ , is given by,

$$\Phi = \sum_n \chi_n(\{R\}) \Psi_n(\{r\}, \{R\}) \quad (4)$$

$$[T_{ion}(\{R\}) + U_{ion}(\{R\}) + E_n] \chi_n(\{R\}) = \omega_n \chi_n(\{R\}). \quad (5)$$

In (5) several small terms have been neglected which involve the action of  $T_{ion}$  on the electronic wave-function. This is a justifiable approximation since these terms have been shown to be of order  $(m/M)^{3/2}$  where  $m$  is the electron mass and  $M$  is the ion mass (see [1]). The ionic wavefunctions must be calculated self-consistently with the electronic wavefunctions as shown in (5).

In order to untangle the electron states from each other, the Hartree or

Hartree-Fock approximation can be employed which decouples the many-electron state into simple, one electron states by the introduction of exchange and correlation energies. The electron-electron interaction  $U_{ee}$  introduces another effect which dresses the remaining coulomb interactions, such as  $U_{ei}$ , with a screening cloud resulting in screened interactions (see section 3). We shall designate this screened electron-ion interaction as  $\tilde{U}_{ei}$ . Similarly, the electron-electron polarization screens other coulomb interactions such as the interaction of conduction electrons (holes) with ionized impurities,  $V_i$ , and the electron-electron (carrier-carrier) interaction between conduction electrons or between conduction electrons and valence electrons,  $V_{ee}$ .  $V_i$  and  $V_{ee}$  are assumed weak and treated as the perturbations responsible for ionized impurity scattering and impact ionization (the inverse Auger process) discussed in later sections of this chapter.

The many electron state is retrieved by placing electrons into the one electron states obeying the Pauli exclusion principle. This is the essence of the one-electron approximation for which,

$$\left[ T_{ei}(r) + \tilde{U}_{ei}(r, \{R\}) + U_{EX} \right] \psi_n(r, \{R\}) = E_n(\{R\}) \psi_n(r, \{R\}), \quad (6)$$

where  $U_{EX}$  is the exchange energy.

The electron mobilities are generally large in most semiconductors, and it is appropriate to treat the electron-ion interaction  $\tilde{U}_{ei}$  as a perturbation [2]. Furthermore, because ionic vibrations involved are relatively small, a good choice for a perturbation approach to decouple the electrons from the ions is an expansion in the displacements of the ions from their equilibrium positions  $u^\alpha(R_l)$ . If these equilibrium positions are designated as  $\{R^0\}$ , the solution of (6) for the one-electron wave-functions yields the familiar Bloch wave-functions of band index  $n$  and wave-vector  $k$ :

$$\begin{aligned} \left[ T_{ei}(r) + \tilde{U}_{ei}(r, \{R^0\}) + U_{EX} \right] \psi_{nk}(r) &= E_n(k) \psi_{nk}(r) \quad (7) \\ H_e(r) \psi_{nk}(r) &= E_n(k) \psi_{nk}(r), \quad \psi_{nk}(r) = u_{nk}(r) e^{ik \cdot r}. \end{aligned}$$

Labeling the equilibrium lattice sites by  $R_l^0$  for integers  $l$ , the basis vectors  $\alpha$ , and keeping only the first two terms in the expansion of  $\tilde{U}_{ei}(r - R_l)$ ,

$$\tilde{U}_{ei}(r - R_l) \approx \tilde{U}_{ei}(r - R_l^0 - \alpha) + u^\alpha(R_l) \cdot \nabla_{R_l} \tilde{U}_{ei}(r - R_l) \Big|_{R_l=R_l^0+\alpha}, \quad (8)$$

the one electron crystal Hamiltonian in the adiabatic approximation becomes:

$$\begin{aligned} H_{1e\alpha} &= T_{ei} + V_e(r) + V_p(r, R) + V_i(r) + V_{ee}(r, r') \quad (9) \\ V_p(r) &= \sum_{l\alpha} u^\alpha(R_l) \cdot \nabla_{R_l} \tilde{U}_{ei}(r - R_l - \alpha) \end{aligned}$$

Here,  $V_e(r)$  is the equilibrium periodic crystal potential,  $\tilde{U}_{ei}(r, \{R^0\})$ .  $V_p(r)$  represents the phonon scattering perturbation.

The ion eigen-states are, (to second order in the ion-ion interaction)

harmonic oscillator states or phonons. Specifically, the ion Hamiltonian is diagonalised by appealing to the raising and lowering operators for the normal modes of vibration, the phonon modes of the crystal. In the phonon occupation number basis, [3]

$$H_i = \frac{1}{2} \sum_{qj} \hbar \omega_j^q (a_j(q) a_j^\dagger(q) + a_j^\dagger(q) a_j(q)), \quad (10)$$

where  $a_j^\dagger(q)$  and  $a_j(q)$  are the raising and lowering operators for the phonon mode of wavevector  $q$  and branch  $j$ . In this notation,  $u^\alpha(R_i)$  can be expressed by an expansion over the normal modes of wavevector  $q$  of the lattice as [4]

$$u^\alpha(R_i) = \sum_{qj} \left[ \frac{\hbar}{2N m_\alpha \omega_j^q} \right]^{\frac{1}{2}} e^{iq \cdot (R_i + a)} [a_j(q) + a_j^\dagger(-q)] \xi_{qj}^1 \quad (11)$$

where  $N$  is the number of primitive cells in the lattice,  $m_\alpha$  is the mass of the ion at basis location  $\alpha$ , and  $\xi_{qj}^1$  is the phonon wavevector.

## 2 Scattering in the Semi-classical Boltzmann Equation

To derive the expressions for scattering in the semi-classical Boltzmann equation (SCBE), we start with the equation of motion for the density matrix  $\rho$  for the adiabatic crystal. As discussed in section 1, the crystal system can be separated into a carrier part (conduction electrons or holes) and a phonon part. The phonons are considered to be a thermodynamic heat bath in equilibrium at some temperature  $T$ . Then, weakly coupled to it are the carriers which we can enumerate with the Bloch wavevector and band index quantum numbers. Furthermore, the carriers are weakly coupled to each other,  $V_{ee}$ , and to impurities,  $V_I$ . As noted above, these interactions are weak, and we can approximate the full density matrix as a product of the carrier density matrix and the equilibrium phonon density matrix at all times. This derivation ignores  $V_{ee}$  so that simple one-particle states can be used; however, to include  $V_{ee}$  to first order, two particle antisymmetrized states can be chosen instead. For one-particle states, the carrier density matrix is labeled only by the wavevector  $k$  ( $\rho_{k\lambda}$ ) (suppressing  $n$ ) and the phonon bath density matrix by  $\rho_B = e^{-\beta H_B}$ . Here,  $\beta = 1/k_B T$ , where  $k_B$  is Boltzmann's constant, and  $H_B = H_i$ , the bath (ionic) Hamiltonian given above. In general, the quantum analogue of the phase space distribution function is the Wigner distribution which is a transformation of  $\rho$ . To demonstrate the form of the scattering kernel ("collision integral") in the SCBE, the field can be ignored and it is permissible to identify the diagonal of  $\rho_{k\lambda}$  as the distribution function  $f(k)$  which occurs in the classical Boltzmann equation.

First, the standard quantum Liouville equation neglecting the electric

field is:

$$i\hbar \frac{\partial \rho}{\partial t} = H_{tot}^* \rho, \quad (12)$$

where the hyper-operator notation

$$A^* B \equiv [A, B] = AB - BA \quad (13)$$

has been employed and  $A$  and  $B$  are operators.  $H_{tot}$  is the adiabatic Hamiltonian as derived in section 1.

The projection operator method (see for example Kubo [5]) separates the diagonal of the system density matrix so that an equation for the time evolution of  $\rho_{kk}^e = f(k)$  is obtained. Then, the two projection operators

$$P = \frac{e^{-\beta H_B} \text{tr}_B}{\text{tr}_B e^{-\beta H_B}} \otimes \delta_{k',k} \quad (14)$$

$$Q = 1 - P \quad (15)$$

with the properties  $PP = P$ ,  $QQ = Q$ , and  $PQ = QP = 0$ , can be used in order to derive equations of motion for the diagonal and off-diagonal parts of  $\rho$  in terms of each other. Here,  $\text{tr}_B$  is the many body trace over the phonon bath states. The projection operator  $P$  projects the portion of  $\rho$  which is diagonal in the carrier quantum numbers (containing the probability of occupancy of the carrier stationary states) and leaves the phonon bath in its equilibrium configuration.

By substitution, we arrive at an equation for only the diagonal part in the form,

$$i\hbar \left( P \frac{\partial \rho}{\partial t} \right) = -\frac{i}{\hbar} P(H_p)^* \int_0^t dt' e^{-\frac{i}{\hbar} Q(H_{tot})^*} Q(H_p)^* (P\rho(t')) \quad (16)$$

where the density matrix has been assumed to be diagonal at  $t = 0$ . Here, all the perturbations discussed earlier have been included in  $H_p$ .

Then, noting the hyper-operator identity for operators  $A$  and  $B$ ,

$$e^{A^*} B = e^A B e^{-A} \quad (17)$$

and that

$$e^{\frac{i}{\hbar} H_{tot}(t-t')} = U_s(t, t') \quad (18)$$

where  $U_s(t, t')$  is the Schroedinger picture propagator for the full Hamiltonian from  $t$  to  $t'$ , we can write equation (16) in terms of these propagators [11],

$$\frac{\partial}{\partial t} P\rho(t) = -\frac{i}{\hbar} P(H_p)^* \int_0^t dt' U_s(t, t') (H_p)^* P\rho(t') U_s(t', t). \quad (19)$$

Since  $H_p$  is considered weak, it can be neglected in the exponential of (18) compared to  $H_B$  and  $H_0 = T_{el} + V_c$ . This allows an expression of  $U_s$  in

terms of products of the free propagators for the bath and the carriers,

$$U_s(t, t') \approx e^{-\frac{i}{\hbar} H_s(t-t')} e^{-\frac{i}{\hbar} H_B(t-t')}. \quad (20)$$

If the matrix element for the electron phonon interaction given in (10) is defined as,

$$(V_p)_{kk'} \equiv \langle n'k' | V_p(r) | nk \rangle, \quad (21)$$

where the phonon operators in  $u^a(R_i)$  have produced to  $N_{jq}$  as discussed above, and the matrix element for the non-phonon scattering terms is defined as

$$(V_i)_{kk'} \equiv \langle n'k' | V_i(r) | nk \rangle \quad (22)$$

for the  $i^{\text{th}}$  perturbation, then the equation of motion for  $\rho_{kk}^a = f(k)$  is given by,

$$\begin{aligned} \frac{\partial}{\partial t} f(k, t) = & \quad (23) \\ & \frac{2Re}{\hbar^2} \sum_{k'} | (V_i)_{kk'} |^2 \int_0^t [T_i(k', k; t') f(k', t') - T_i(k, k'; t') f(k, t)] dt' + \\ & \frac{2Re}{\hbar^2} \sum_{k'} | (V_p)_{kk'} |^2 \int_0^t [T_p(k', k; t') f(k', t') - T_p(k, k'; t') f(k, t')] dt' \end{aligned}$$

with

$$T_i(k, k') = e^{-i(\omega(k) - \omega(k'))(t-t')} \quad (24)$$

$$\begin{aligned} T_p(k, k') = & (N_{k-k'} + 1) e^{-i(\omega(k) - \omega(k') - \omega_{k-k'})(t-t')} + \\ & (N_{k-k'}) e^{-i(\omega(k) - \omega(k') + \omega_{k-k'})(t-t')}, \quad (25) \end{aligned}$$

with  $\omega(k) \equiv E(k)/\hbar$ .  $T_i(k, k')$  and  $T_p(k, k')$  are functions associated with non-phonon and phonon scattering from  $k$  to  $k'$  respectively. Furthermore, the trace over the phonons and the action of the raising and lowering operators in the electron-phonon perturbation have produced the factors  $N_{jq} + 1$  and  $N_{jq}$  for emission and absorption respectively with  $N_{jq}$  being the Bose-Einstein average occupation number for the phonon of wavevector  $q$  and phonon branch  $j$ :

$$N_{jq} = \frac{1}{e^{\hbar\beta\omega_{jq}} - 1}. \quad (26)$$

If  $f(t)$  were outside of the time integrals, the integral over  $t$  of the  $T(k, k')$  becomes the familiar delta functions of energy conservation. For example,

$$\lim_{t \rightarrow \infty} \int_0^t dt' Re(T_i(k, k'; t')) \rightarrow \pi \hbar \delta(E(k) - E(k')). \quad (27)$$

Since  $f(t)$  typically changes very little in the time it takes to establish a delta function,  $f(t)$  can indeed be taken outside of the time integral. The result is the standard Boltzmann equation with the scattering rate

$S(k, k')$  from  $k$  to  $k'$  given by the familiar Golden Rule expression for energy conservation:

$$S_i(k, k') = \frac{2\pi}{\hbar} |(V_i)_{kk'}|^2 \delta(E(k) - E(k')) \quad (28)$$

for elastic scattering processes, and

$$S_p(k, k') = \frac{2\pi}{\hbar} (N_q + \frac{1}{2} \pm \frac{1}{2}) |(V_p)_{kk'}|^2 \delta(E(k) - E(k') \mp \omega_q) \quad (29)$$

for phonon scattering processes where the upper sign is taken for emission and the lower sign for absorption and  $q = k - k'$ . Thus, the scattering rates in the SCBE are simply given by the Fermi Golden Rule from quantum mechanics.

However, the scattering events have been treated as if they happened instantaneously as a result of the approximation in (27). This approximation breaks down in three cases. The first case is obvious. If transients are to be resolved on a time scale of the order of the time it takes to establish (27) and the scattering rates are high,  $f(k, t)$  cannot be pulled out of the time integral and the simple forms in (28) or (29) will not apply. If the perturbations are sufficiently weak, then  $f(k, t)$  can still be removed from the time integral, but (28) and (29) must be replaced with partially completed delta functions, which relax energy conservation. This is just a manifestation of the energy and time uncertainty principle.

Second, if scattering rates are high, the approximation of a weak interaction leading to equation (18) breaks down, and in the time it takes to establish the delta function in (27), the original state can decay appreciably. To account for the depletion of the initial state in the finite time it takes for the collision to become "complete" the approximation in (18) must be improved to include the effect of  $H_p$  in  $U_s(t, t')$ . One way to account for  $H_p$  is to calculate the full propagator  $U_s(t, t')$  from field theory. This leads to two additions to (23). First, the simple propagators in the scattering terms are dressed by virtual transitions in the self-energy  $\Sigma(k, E)$  [6]. The second addition unfortunately leads to the inclusion of terms which do not resemble the Boltzmann equation. Typically these terms are assumed small and are ignored. At present, it is unclear what effect these terms have. Following the general approach that these terms are small, we can augment the SCBE by including  $\Sigma(k, E)$  in equation (18).

Assuming that the self-energy can be calculated, (see for instance reference [7] for a self-consistent calculation of the self-energy for realistic band structures) quantum field theory states that for  $t > t'$  [6],

$$U_s(k; t, t') = e^{-\frac{i}{\hbar}(E(k) + \Delta(k))(t-t')} e^{-\frac{1}{\hbar}(\Gamma(k))(t-t')}, \quad (30)$$

with

$$\begin{aligned} \Delta(k) &= \text{Re}(\Sigma(k)) \\ \Gamma(k) &= \text{Im}(\Sigma(k)) . \end{aligned} \quad (31)$$

Physically,  $\Delta(k)$  corresponds to a shift in the energy level  $E(k)$ , and  $\Gamma(k)$  corresponds to the finite lifetime of the state  $k$ . For example, the probability that a particle which starts at time  $t'$  in state  $k$  is in state  $k$  at time  $t$  ( $t \geq t'$ ) is

$$|U_s(k; t, t')|^2 = e^{-\frac{1}{\hbar} \Gamma(k)(t-t')}. \quad (32)$$

The total scattering rate out of state  $k$ ,  $S_{tot}(k)$ , can be identified as

$$S_{tot}(k) = \frac{2}{\hbar} \Gamma(k), \quad (33)$$

by interpreting the lifetime of the state as the inverse of the total scattering rate. (This can also be shown through application of the Optical Theorem of quantum mechanics [8].) This clearly demonstrates the connection between high scattering rates and the finite lifetime of the state.

When (32) is substituted into (23), the limit in equation (27) becomes,

$$A(E, E') \equiv \quad (34)$$

$$\lim_{t \rightarrow \infty} \text{Re} \int_0^t dt' e^{-\frac{1}{\hbar} (E(k) + \Delta(k) - E(k') + \Delta(k'))(t-t')} e^{-\frac{1}{\hbar} (\Gamma(k) + \Gamma(k'))(t-t')}$$

$$= \frac{\hbar}{\pi} \frac{\Gamma(E) + \Gamma(E')}{(E + \Delta(E) - E' - \Delta(E'))^2 + (\Gamma(E) + \Gamma(E'))^2}.$$

Therefore, one way to add the effects of high scattering rates to the SCBE is to replace  $\delta(E - E')$  with  $A(E, E')$  which is the familiar Lorentzian line shape. The effect of broadening the delta function through high scattering rate is termed *collision broadening*.

Lastly, if a large electric field is present, the carriers can be accelerated appreciably during the time of the collision. This is referred to the *intracollisional field effect*. In general, this effect can also broaden the energy conserving delta function, however, it is more difficult to deal with in a compact way. The interested reader is referred to the following references for a detailed treatment of this effect and collision broadening: [9]-[11]. Also, for an overview of attempts to include collision broadening and the intracollisional field effect in Monte Carlo Simulations see: [12]-[13].

### 3 Dielectric Screening

As discussed in section 1, the scattering potentials  $V_{ee}$ ,  $V_i$  and  $V_p$  are self-consistent, screened potentials which result from bare perturbations. Because in most cases the bare potentials are simple Coulomb potentials,  $v(q) = 1/(4\pi\epsilon_0 q^2)$ , the easiest way to calculate the self-consistent perturbations is to screen the bare perturbations with the dielectric function which connects the two.

Suppose the potential,  $V_{en}(r, t)$  is introduced as a bare, external potential to the crystal. The resulting (true) potential felt at time  $t'$  and position  $r'$  is  $V_{tr}(r', t')$  and the induced charge is  $\rho_{in}(r, t)$ . If  $V_{en}$  is weak enough that first order perturbation theory is adequate, then we can calculate the

redistribution of charge,  $\rho_{in}(r, t)$  as a linear functional of the self-consistent potential  $V_{ir}(r, t)$ . In general [18]

$$\rho_{in}(r, t) = \int d^3r' \int dt' \chi(r, r'; t - t') V_{ir}(r', t') \quad (35)$$

where  $\chi(r, r'; t - t')$ , the electronic susceptibility, is calculated from first order perturbation theory in which  $V_{ir}$  is the perturbation. A related quantity called the dielectric function can similarly be defined:

$$V_{en}(r, t) = \int d^3r' \int dt' \epsilon(r, r'; t - t') V_{ir}(r', t'). \quad (36)$$

The "inverse" of the dielectric function is the quantity we want since it expresses the true potential in terms of the bare (external) potential.

The Fourier transform  $\rho(q + G, \omega)$  of equation (35) can be written,

$$\rho_{in}(q + G, \omega) = \int_{Vol} d(q' + G') \chi(q + G, q' + G'; \omega) V_{en}(q' + G', \omega), \quad (37)$$

where  $G$  is a reciprocal lattice vector,  $q$  is a wavevector in the first Brillouin zone (BZ), and  $Vol$  is the crystal volume. Because  $\chi$  is lattice translationally invariant,  $\chi(r, r') = \chi(r + R_j, r' + R'_j)$ , and the integral in equation (35) becomes a summation: [14]

$$\rho_{in}(q + G, \omega) = \sum_{G'} \chi(q + G, q + G', \omega) V_{ir}(q + G', \omega). \quad (38)$$

A similar result holds for  $\epsilon(q + G, q + G', \omega)$ :

$$V_{en}(q + G, \omega) = \sum_{G'} \epsilon(q + G, q + G', \omega) V_{ir}(q + G', \omega). \quad (39)$$

Application of Poisson's equation connects  $V_{ir}$  with  $V_{en}$  [16] Fourier transforming the Poisson's equations for the total charge  $\rho = \rho_{in} + \rho_{en}$  and the external charge  $\rho_{en}$  we have,

$$(q + G)^2 V_{ir}(q + G, \omega) = -\frac{1}{\epsilon_0} \rho(q + G, \omega) \quad (40)$$

$$(q + G)^2 V_{en}(q + G, \omega) = -\frac{1}{\epsilon_0} \rho_{en}(q + G, \omega). \quad (41)$$

Solving (40) and (41) for  $\rho_{in}$  and substituting this into (38) identifies the dielectric function in (39) as:

$$\epsilon(q + G, q + G', \omega) = \delta_{GG'} - \frac{1}{\epsilon_0(q + G)^2} \chi(q + G, q + G', \omega). \quad (42)$$

The random phase approximation (RPA), a type of first order perturbation calculation including the temperature through the distribution function

$f_n(k)$ , defines  $\chi$  as:

$$\chi^e(q+G, q+G', \omega) = \sum_{nn'h} \frac{f_{n'}(k+q) - f_n(k)}{E_{n'}(k+q) - E_n(k) + \hbar\omega} \\ \langle nk | e^{-i(\tau+G)\cdot r} | n'(k+q) \rangle \langle n'(k+q) | e^{i(\tau+G')\cdot r} | nk \rangle. \quad (43)$$

This together with (42) expresses the effects of screening on a bare, external potential. Then, the inverse of the matrix  $\epsilon(q+G, q+G')$ , where the rows and columns are labeled by  $G$  and  $G'$ , expresses the true perturbations  $V_{ee}$ ,  $V_i$  and  $V_p$  in terms of the bare Coulomb potentials which give rise to the perturbations. A plot of  $\epsilon(q, q)$  is shown in figure 1 as a function of  $\omega$  for silicon at zero temperature calculated using equation (43).

Several simplifications of this result are applicable for scattering in semiconductors. First, the off-diagonal terms can usually be neglected for non-phonon scattering since they are usually smaller than the diagonal. They must be kept for phonon scattering since they are necessary to fulfill certain sum rules ([2]). Furthermore, since there are usually many more electrons in the valence bands than there are electrons (holes) in the conduction (valence) bands,  $f_n(k) \approx 1$  for valence bands and  $f_n(k) \approx 0$  for conduction bands. This is the zero temperature approximation.

One simple way to include the effect of the free conduction band electrons in the  $T=0$  model is to add the susceptibilities for the  $T=0$  case,  $\chi^0$  and the susceptibility for a free electron gas  $\chi^e$  with density equal to the density of conduction band electrons. Two expressions for  $\chi^e$  are given by the Thomas-Fermi screening theory and the Lindhard screening theory for a free electron gas [17]. For example, in the Thomas-Fermi theory

$$\chi^e(q) = -e^2 \frac{\partial f_0(E, E_f)}{\partial E_f} \quad (44)$$

where  $f_0$  is an equilibrium Fermi distribution in the conduction bands, and  $E_f$  is the Fermi energy. Then, a natural screening length can be defined as

$$k_{TF}^2 = \frac{e^2}{\epsilon_0} \frac{\partial f_0(E, E_f)}{\partial E_f}, \quad (45)$$

so that

$$\epsilon(q) = 1 + \frac{k_{TF}^2}{q^2}. \quad (46)$$

Having derived relations between the bare perturbing potentials and the screened potentials which result, we can explicitly calculate important scattering matrix elements for use in the SCBE of section 2.

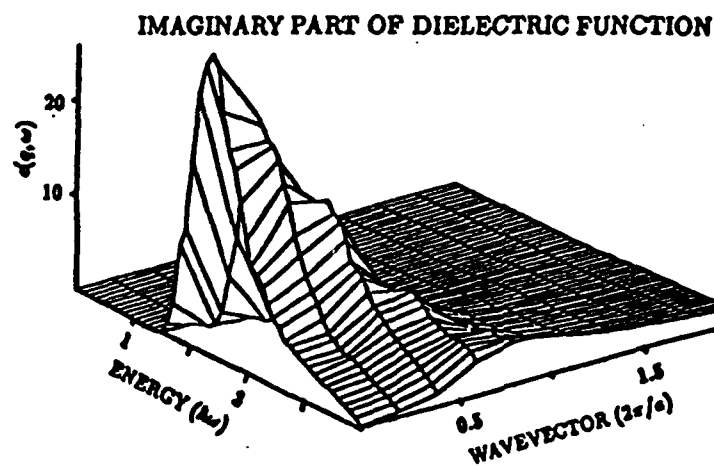
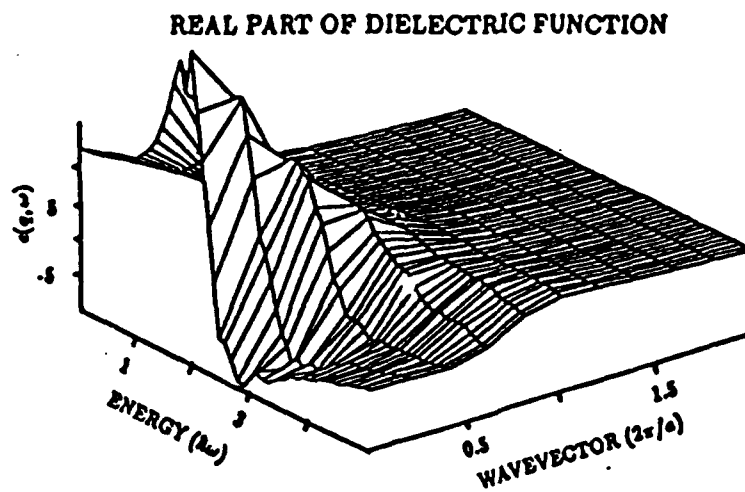


Figure 1: Real and Imaginary parts of the frequency and wavevector dependent dielectric function in silicon calculated using the random phase approximation (RPA).

## 4 Phonon Scattering

### 4.1 Phonon Perturbation Potential

In this section, the phonon perturbation is rewritten in terms of the bare potential and the dielectric function, and the matrix elements  $(V_p)_{n,n',n,k}$  from (21) are calculated. From section 1, the perturbing potential was found to be

$$V_p(r) = \sum_{I\alpha} u^\alpha(R_I) \cdot \nabla_{R_I} \tilde{U}_{\alpha I}(r - R_I - \alpha) \quad (47)$$

where  $\tilde{U}_{\alpha I}(r - R_I - \alpha)$  is the self-consistent pseudopotential (effective potential outside of the ion itself) felt by an electron at  $r$  due to the ion at site  $R_I$  and basis vector  $\alpha$ , and  $\nabla_{R_I} \cdot \tilde{U}_{\alpha I}(r - R_I)$  is the local gradient of that pseudopotential taken with respect to the ionic location. Proceeding as in Vogl [2], we Fourier transform  $V_p(r)$ :

$$V_p(r) = \sum_{qG} e^{i(q+G)\cdot r} \partial V(q+G), \quad (48)$$

where,  $q$  is a vector in the first Brillouin zone and  $G$  is a reciprocal lattice vector. The summation above must contain all vectors of reciprocal space because  $V_p(r)$  depends on the displacements  $u^\alpha(R_I)$  which are not in general periodic in a primitive lattice translation. Since the displacements are small, we assume that  $\tilde{U}_{\alpha I}$  is related to the unscreened ionic potential  $v_\alpha$  by the inverse dielectric function  $\epsilon^{-1}(r, r')$  as described in section 3. In this context the unscreened ionic pseudopotential,  $v_\alpha$ , is the potential of the nucleus and the core electrons associated with the basis ion  $\alpha$ . If the crystal is monoatomic,  $v_\alpha$  is independent of  $\alpha$ .  $v_\alpha$  behaves like a Coulomb potential at long distances, but has a repulsion for short distances due to the core electrons (see [17]). A more exact expression for this potential is given in the chapter by Fischetti and Higman.

In terms of the bare pseudopotential and the dielectric function,

$$\begin{aligned} \partial V(q+G) &= \frac{1}{V\alpha} \int_{V\alpha} d^3r e^{-i(q+G)\cdot r} \sum_{I\alpha} u^\alpha(R_I) \cdot \\ &\int_{V\alpha} d^3r' \epsilon^{-1}(r, r') \nabla_{R_I} v_\alpha(r' - R_I - \alpha), \end{aligned} \quad (49)$$

where  $V\alpha$  is the crystal volume. The resulting Fourier components,  $\partial V(q+G)$ , of the screened perturbation are referred to as pseudopotential perturbations.

From section 3 we can write equation (50) in reciprocal lattice space as,

$$\begin{aligned} \partial V(q+G) &= -i \sum_{I\alpha} u^\alpha(R_I) \cdot \\ \sum_{G'} \epsilon^{-1}(q+G, q+G')(q+G') e^{i(R_I+\alpha)\cdot(q+G')} v_\alpha(q+G'). \end{aligned} \quad (50)$$

The result of equation (50) comes from the recognition that  $\nabla_{R_l} v_a(r - R_l - \alpha) = -\nabla_r v_a(r - R_l - \alpha)$ , and an application of the shifting and derivative properties of the Fourier transform. We do not need to consider the frequency dependence in (50) since in the adiabatic approximation, the ions are assumed to be stationary.

Substituting the expression in equation (11) for  $u^a(R_l)$  into equation (50), we can write,

$$\partial V(q+G) = \frac{-i}{V\alpha} \sum_{ajq'G'} \left[ \frac{\hbar}{2Nm_a\omega_j^2} \right]^{\frac{1}{2}} [a_j(q') + a_j^\dagger(-q')] \xi_{aj}^2 \cdot \quad (51)$$

$$(q+G')\epsilon^{-1}(q+G, q+G')v_a(q+G')e^{-i(q+G')\cdot\alpha} \sum_l e^{i(q'-q-G')\cdot R_l}$$

Concentrating on the sum over  $l$ , we can make several simplifications. First,  $G'\cdot R_l$  is always  $2\pi$ , so the  $G'$  in the first exponential can be ignored. Second, if  $q' \neq q+G''$  with  $G''$  being any reciprocal lattice vector, the sum vanishes because

$$\sum_l e^{iR_l\cdot(q-q')} = N\delta_{q, q'+G''} \cdot \quad (52)$$

Hence, we can considerably simplify equation (51) and write it as

$$\partial V(q+G) = \frac{-i}{\Omega} \sum_{ajq'} \left[ \frac{\hbar}{2Nm_a\omega_j^2} \right]^{\frac{1}{2}} [a_j(q) + a_j^\dagger(-q)] \xi_{aj}^2 \cdot \quad (53)$$

$$(q+G')\epsilon^{-1}(q+G, q+G')v_a(q+G')e^{-i\alpha\cdot q}$$

where the fact that  $\Omega = V\alpha/N$ , the unit cell volume, has been used. Equation (53) is substituted into equation (48) to give the full electron-phonon perturbation  $V_p(r)$  in terms of the bare ion pseudopotential and the dielectric function.

#### 4.2 General Electron-Phonon Matrix Elements

To calculate the matrix elements of the electron-phonon interaction as required in the scattering kernel (see section 2, equation (29)), we need only calculate the matrix element of  $e^{i(\epsilon+G)\cdot r}$  between Bloch states. For example,

$$\langle n'k' | V_p(r) | nk \rangle = \sum_{qG} \partial V(q+G) \langle n'k' | e^{i(\epsilon+G)\cdot r} | nk \rangle \cdot \quad (54)$$

where  $|nk\rangle$  are the normalised Bloch states  $N^{-\frac{1}{2}}u_{nk}(r)e^{ik\cdot r}$  of band index  $n$  and wave vector  $k$ . The phonon raising and lowering operators in equation (53) have already acted on the phonon occupation states to give  $N_{aj}$  as in section 2, equation (26). The electronic part of the matrix

element provides conservation of the total crystal momentum as follows:

$$\langle n'k' | e^{i(q+G)\cdot r} | nk \rangle = \frac{1}{N} \int_{V_{cd}} u_{n',k'}^*(r) u_{nk}(r) e^{i(k'-k)\cdot r} e^{i(q+G)\cdot r} d^3r \quad (55)$$

$$= \delta_{k',k\pm q+G'} \int_{\Omega} u_{n',k'}^*(r) u_{nk}(r) e^{i(\mp G-G')\cdot r} d^3r \quad (56)$$

Here, the integral in (55) was factored into a sum of integrals over the primitive cell. The result of (56) follows from the identity given in (52). The  $G'$  in the Kronecker delta refers to a general reciprocal lattice vector, not necessarily the particular  $G$  in the integral. When  $G' \neq 0$ , the scattering process is called an Umklapp process (assisted by a reciprocal lattice vector). In the following sections,  $\delta_{k',k\pm q}$  always implies that Umklapp processes are allowed ( $\delta_{k',k\pm q} \rightarrow \delta_{k',k\pm q\pm G'}$ ), although the  $G'$  will be suppressed in the notation. If an Umklapp process occurs, then an extra term,  $e^{iG'\cdot r}$ , appears in each integral.

### 4.3 Phenomenological Phonon Scattering Processes

The form of the electron-phonon matrix element as given in (54), written in terms of microscopic quantities is exact within the rigid-pseudo-ion approximation (see the chapter in this book by Fischetti and Higman) [19]. However, because it requires a detailed knowledge of both the dielectric matrix and the Bloch wavefunctions, it is very difficult to calculate. With some approximations, simple forms for these interaction matrix elements which correspond to well known phenomenological scattering processes in semiconductors can be demonstrated [2]. In particular, the acoustic and optical deformation potentials and the polar optic interactions can be extracted from (54), and the approximations leading to these familiar processes can be examined.

From equation (53) it is apparent that  $V_p(r)$  can contain both *long range* and *short range* components. Long-range components vary negligibly within the unit cell and produce fields, whose average over many cell lengths does not vanish. The long-range components are therefore responsible for the macroscopic fields produced in the crystal, which have been identified with the phenomenological polar optic interaction in polar materials, and the piezoelectric interaction in both polar and nonpolar materials ([2]). In contrast, the short-range components of the perturbing potential involve rapid oscillations within the unit cell, and consequently, their average on any macroscopic length scale vanishes. They do, however, contribute to scattering through the phenomenological deformation potential interaction.

The separation of  $V_p(r)$  into short and long-range components has been shown by Vogl by considering the behavior of  $\partial V(q+G)$  as  $q \rightarrow 0$  [2]. We

quote only the result,

$$V_p(\mathbf{r})_{lr} = e^{i\mathbf{q}\cdot\mathbf{r}} \left[ 1 + \sum_{\mathbf{G} \neq 0} e^{i\mathbf{G}\cdot\mathbf{r}} \frac{e^{-i(\mathbf{q}+\mathbf{G})\cdot\mathbf{r}}}{e^{-i\mathbf{q}\cdot\mathbf{r}}} \right] \partial V(\mathbf{q}) \quad (57)$$

$$V_p(\mathbf{r})_{sr} = \sum_{\mathbf{G} \neq 0} e^{i(\mathbf{q}+\mathbf{G})\cdot\mathbf{r}} \partial V(\mathbf{q}+\mathbf{G}), \quad (58)$$

where  $V_p(\mathbf{r})_{lr}$  and  $V_p(\mathbf{r})_{sr}$  are the long and short range components respectively.

#### 4.3.1 Phenomenological Deformation Potential

The electron-phonon matrix element for the short-range interaction is obtained by combining equations (58), (53) and (55). The resulting matrix element can be recast into the form of the deformation potential interaction, and will be shown to involve, for small  $q$ , dilation for optical modes and elastic strain for acoustic modes. For large  $q$ , the form of the phenomenological intervalley scattering matrix element will be discussed.

We start by putting  $\langle n'k' | V_p(\mathbf{r})_{sr} | nk \rangle$  into a more manageable form for a crystal with a basis of two ( $\alpha = 1$  and  $\alpha = 2$ ). For a crystal with a basis there are two phonon types, *optical* and *acoustic*, and they behave quite differently. For acoustic modes,  $\lim_{q \rightarrow 0} \omega(\mathbf{q}) \rightarrow 0$ , corresponding to a rigid displacement of the entire lattice, whereas, for optic modes,  $\lim_{q \rightarrow 0} \omega(\mathbf{q}) \rightarrow \omega_{op} \neq 0$  corresponding to rigid displacement of the two sublattices. The latter case can cause transitions between the adiabatic Bloch states leading to scattering, but the former case cannot lead to scattering [20]. For small  $q$  it is possible to write the phonon polarisation vectors,  $\xi_{\alpha j}^{\mathbf{q}}$ , as  $\xi_{1j}^{\mathbf{q}} = Km_1^{1/2} \hat{\xi}_{j\mathbf{q}}$  and  $\xi_{2j}^{\mathbf{q}} = \pm Km_2^{1/2} \hat{\xi}_{j\mathbf{q}}$  where  $\hat{\xi}_{j\mathbf{q}}$  is a unit vector,  $K$  is a constant, and the plus (minus) sign is chosen for acoustic (optical) modes. Furthermore, in this limit, there are three acoustic and three optical branches corresponding to two modes polarised transversely to the direction of propagation and one polarised longitudinally.

$$\langle n'k' | V_p(\mathbf{r})_{sr} | nk \rangle = \left( N_{j\mathbf{q}}(T) + \frac{1}{2} \pm \frac{1}{2} \right) \left[ \frac{\hbar}{2N\mu\omega_{j\mathbf{q}}} \right]^{\frac{1}{2}} \quad (59)$$

$$-i \delta_{k', k \pm \mathbf{q}} \langle n'k' | e^{-i\mathbf{q}\cdot\mathbf{r}} V_{j\mathbf{q}}^{sr}(\mathbf{r}) | nk \rangle \hat{\xi}_{j\mathbf{q}}$$

with  $V^{sr}$  given by comparison with (58) and (53).  $\mu$  can be chosen to be the reduced mass. Since, the final form for (59) is phenomenological, the constant can be chosen to accommodate the choice of  $\mu$ .

To compare (59) with the phenomenological forms for deformation potential scattering, we expand  $e^{i\mathbf{q}\cdot\mathbf{r}}$  in a Taylor series in  $q$  and look for the highest order non-vanishing terms.

For small  $q$ , the exponential in equation (59) can be expanded as  $e^{i\mathbf{q}\cdot\mathbf{r}} \approx 1 + i\mathbf{q}\cdot\mathbf{r}$ . For the acoustic phonon case, the highest order term in (59) which

does not vanish is the  $q \cdot r$  term, since as discussed above, the constant term corresponds to a rigid displacement of the entire crystal which cannot scatter [2]. For a particular mode  $j$ , (59) then becomes

$$\begin{aligned} \langle n'k' | V_p(r)_{,rr} | nk \rangle_{ac} &= \left( N_{jq}(T) + \frac{1}{2} \pm \frac{1}{2} \right)^{\frac{1}{2}} \\ \delta_{k',k \pm q} \langle n'k' | (q_x r_x + q_y r_y + q_z r_z) V_{,rr}(r) | nk \rangle &= \xi_{jq} \end{aligned} \quad (60)$$

Equation (60) can be put in the form of the familiar deformation potential interaction as first expressed by Shockley, which for a given phonon branch is [21]-[23],

$$\begin{aligned} \langle n'k' | V_p(r)_{,rr} | nk \rangle_{ac} &= \\ \delta_{k',k \pm q} \left[ \frac{\hbar}{2N\mu\omega_j} \right]^{\frac{1}{2}} \left( N_{uj}(T) + \frac{1}{2} \pm \frac{1}{2} \right)^{\frac{1}{2}} \sum_u \Xi_{uj} S_{uj} \end{aligned} \quad (61)$$

The terms in (60) correspond to the following terms from (61):

$$\Xi_{uj} = \langle n'k' | [(V_j^{,rr})_{,i} r_i + (V_j^{,rr})_{,i} r_i] | nk \rangle \quad (62)$$

where  $(V_j^{,rr})_{,i}$  is the  $i^{\text{th}}$  component of  $V_j^{,rr}$ , and

$$S_{ij} = \frac{1}{2}(\xi_i q_j + \xi_j q_i) = \frac{1}{2} \left( \frac{\partial u_i}{\partial x_j} + \frac{\partial u_j}{\partial x_i} \right) \quad (63)$$

Since the displacement,  $u$ , is proportional to  $\xi_j e^{iq \cdot r}$ ,  $S_{ij}$  is the elastic strain tensor [25]. Thus,  $\Xi_{uj}$  is the deformation potential tensor which couples the local strain set up by the acoustic phonon to the scattering matrix element as given in the phenomenological theories of scattering by acoustic phonons. Equation (61) is valid for small  $q$ , which corresponds to intravalley scattering for low energies and represents the anisotropy of the coupling constant. For larger  $q$ , higher order terms in  $iq \cdot r$  come into the integral in (60), and hence the coupling to the phonon wavevector involves higher rank tensors.

Now, returning to (59) for the case of optical phonons, the highest order term which can be non-zero is the zero-order term. In contrast to the acoustic mode case, the zero-order term can be nonzero because when  $q \rightarrow 0$  for an optic mode, the two sublattices are rigidly displaced with respect to one another, and this can scatter carriers. Thus, for the case of optical phonons, we look to highest order at the zero-order term and write

$$\begin{aligned} \langle n'k' | V_p(r)_{,rr} | nk \rangle_{op} &= \\ -i \left( N_{uj}(T) + \frac{1}{2} \pm \frac{1}{2} \right)^{\frac{1}{2}} \delta_{k',k \pm q} \langle n'k' | V_{jq}^{,rr}(r) | nk \rangle &= \xi_{jq} \end{aligned} \quad (64)$$

This is valid for small  $q$  (intravalley scattering). Equation (64) can also be

written in terms of an optical deformation potential vector  $D_{op}$  as,

$$\langle n'k' | V_p(r)_{,r} | nk \rangle_{op} = \quad (65)$$

$$\left( N_{ij}(T) + \frac{1}{2} \pm \frac{1}{2} \right)^{\frac{1}{2}} \left[ \frac{\hbar}{2N\mu\omega_q^2} \right]^{\frac{1}{2}} D_{op} \cdot \xi_{ij} \delta_{k',k \pm q} \quad (66)$$

The form of the electron-phonon matrix element for small  $q$  and optical modes involves a direct dilation of the local crystal structure as seen from the dot product coupling  $D_{op} \cdot \xi$ . Thus, 66 yields the phenomenological optical deformation potential matrix element ([25]). It has been shown that for symmetry reasons the intravalley optical deformation potential scattering vanishes for X and  $\Gamma_1$  valleys for the zero-order matrix element discussed above [26]-[27]. In general, the higher order tensor coupling (acoustic-like) can be non-zero.

While for small  $q$  the phenomenological form of the deformation potential interaction for acoustic and optic modes is quite different, for large  $q$ , the coupling contains many complicated higher order tensor modes. The standard treatment for these situations assumes that, for a particular intervalley transition (for example, X-X,  $\Gamma$ -X),  $q$  is confined to a small cone of allowed directions. Because the angular orientation is fairly constant within this cone, the tensor coupling can change only a small amount for any scattering into the cone. Then, it may be approximately correct to treat the coupling for intervalley transitions by a constant. Usually the intervalley deformation potential matrix element is written phenomenologically as [24]

$$\langle n'k' | V_p(r)_{,r} | nk \rangle_{iv} = D_{iv} \left[ \frac{\hbar}{2N\mu\omega_q^2} \right]^{\frac{1}{2}} \left( N_{ij}(T) + \frac{1}{2} \pm \frac{1}{2} \right)^{\frac{1}{2}} \delta_{k',k \pm q} \quad (67)$$

Both acoustic and optical modes have been shown to participate in intervalley scattering with this type of scattering rate. It has been shown, for instance, that to fit experimental values of conductivity in silicon, it is necessary to include acoustic phonons in intervalley scattering [28]. It is evident from the nature of the integral in (59) that the coupling is widely determined by the orientation of the final valleys and the phonon branch. Thus, for each phonon branch and each set of initial and final valleys, a new intervalley coupling constant,  $D_{iv}$ , must be chosen. Typically, the values for  $D_{iv}$  are selected to best fit experimental data for a given Monte Carlo simulation [29]-[31].

Finally, for the phenomenological deformation potential interaction, some authors have factored out the overlap integral,

$$I(n'k', nk) = \int_{\Omega} d^3r u_{nk}(r) u_{n'k'}^*(r), \quad (68)$$

from the matrix elements. This is only valid for the long range interaction, as discussed in the next section, and can readily be seen from (56) and (57).

### 4.3.2 The Phenomenological Polar Optical Interaction

In this section, the phenomenological polar optic phonon matrix element will be derived from the long-range matrix element in (57), using the equations of macroscopic electrostatics [2]. The first step is to factor out of (57) all terms proportional to the Coulomb potential  $v(q) \propto 1/q^2$  so that the behavior of the matrix element for small  $q$  is clear. These terms can be factored out giving,

$$\langle n'k' | V_p(\mathbf{r})_{lr} | nk \rangle_{r0} = -iV_m(q)I(n'k', nk) \quad (69)$$

$$V_m(q) \equiv \frac{1}{\Omega} \frac{N_{eff}(T)}{\epsilon(q)q} \sum_{\alpha} Z_{\alpha}^{\dagger} \cdot \xi_{\alpha}^{\alpha},$$

with,

$$N_{eff}(T) \equiv \left( N_{\alpha j}(T) + \frac{1}{2} \pm \frac{1}{2} \right)^{\dagger} \left[ \frac{\hbar}{2N\mu\omega_q^2} \right]^{\dagger}. \quad (70)$$

The quantity  $Z_{\alpha}^{\dagger}$  is the remainder of (57) after the singular  $1/q$  terms are removed (see Vogl [2]). The whole matrix element is proportional to  $1/q$  and so, acts quite differently than the deformation potential matrix element. Here,  $\epsilon(q, q) = \epsilon(q)$ , the macroscopic dielectric function. Equation (69) is a fairly intractable formula, since the function  $Z_{\alpha}^{\dagger}$  is generally difficult to calculate. However, there exists a simple expression for  $Z_{\alpha}^{\dagger}$  which can be seen by using macroscopic electrostatics. This is only possible because of the long-range nature of the perturbation discussed earlier.

The term containing the product  $\xi_{\alpha}^{\alpha} N_{eff}(T)$ , can be treated as the effective phonon polarisation vector,  $\mathbf{u}$ . In addition,  $V_m(q)$  is the true macroscopic potential perturbation set up by this phonon. As such, it can be examined using macroscopic electrostatics and related to the polarisation wave of the phonon.

Two equations from macroscopic electrostatics directly apply: first,

$$\nabla \cdot D(\mathbf{r}) = \nabla \cdot (\epsilon_0 \mathbf{E}(\mathbf{r}) + \mathbf{P}(\mathbf{r})) = 0 \iff \mathbf{E}(q) = -\mathbf{P}(q)/\epsilon_0 \quad (71)$$

in the absence of excess charge (charge neutrality is not necessary for the proof but it is a convenient assumption), and  $\mathbf{P}(q)$  is the polarisation. Second,

$$\nabla \cdot V(\mathbf{r}) = -e\mathbf{E}(\mathbf{r}) \iff iqV(q) = -e\mathbf{E}(q) \cdot \hat{q} \quad (72)$$

where  $V(\mathbf{r})$  is the potential energy felt by an electron. Together these equations give

$$iqV_m(q) = e\hat{q} \cdot \mathbf{P}(q)/\epsilon_0 \quad (73)$$

which can be substituted into (3.25) to give

$$\langle n'k' | V_p(\mathbf{r})_{lr} | nk \rangle_{r0} = \frac{I(n'k', nk)\hat{q} \cdot e\mathbf{P}(q)}{\epsilon_0 q}. \quad (74)$$

Comparing 74 with 69 yields the polarization  $P(q)$  in terms of microscopic quantities.

For small  $q$ ,  $P(q)$  is the dipole polarization set up by the optical phonon mode in the crystal. For larger  $q$   $P(q)$  acquires higher order poles (quadrupole polarization, etc.). We are only interested in the small  $q$  limit for polar optic phonon scattering, so for these purposes,  $P(q) \approx P_{dipole}$ . Fortunately, the dipole polarization associated with a long wavelength mode is easily calculated from a self-consistent, first order lattice dynamics theory. The result is that [32],

$$\mathbf{q} \cdot P_{dipole} = \frac{e_L^* \mathbf{u} \cdot \mathbf{q}}{\Omega}, \quad (75)$$

where  $e_L^*$  is the effective dipole charge associated with a longitudinal optical phonon and  $\mathbf{u}$  is the ionic displacement. Furthermore, an application of the well known Lyddane-Sachs-Teller relation relates the effective charge,  $e_L^*$ , to the experimentally known quantities  $\epsilon_r$ ,  $\epsilon_\infty$  and the longitudinal optical phonon frequency at some center  $\omega_{LO}$  [32]:

$$(e_L^*)^2 = \Omega \epsilon_0 \mu \omega_{LO}^2 \left( \frac{1}{\epsilon_r} - \frac{1}{\epsilon_\infty} \right). \quad (76)$$

This allows us to rewrite (69) for small  $q$  in a more transparent form involving experimentally known quantities:

$$\langle n'k' | V_p(r)_{i\alpha} | nk \rangle_{po} = \frac{e N_{eff}(T) e_L^* \mathbf{q} \cdot \xi_{ij}^\alpha}{\Omega \epsilon_0 q} I(n'k', nk) \quad (77)$$

or, in the familiar Frohlich interaction form,

$$|\langle n'k' | V_p(r)_{i\alpha} | nk \rangle_{po}|_{LO}^2 = I^2(n'k', nk) \quad (78)$$

$$\delta_{k', k \pm q} \left( N_{ij}(T) + \frac{1}{2} \pm \frac{1}{2} \right) \frac{e^2 \hbar \omega_{LO}}{2 \epsilon_0 V \alpha q^2} \left( \frac{1}{\epsilon_r} - \frac{1}{\epsilon_\infty} \right)$$

Pure transverse modes do not scatter because for them,  $\mathbf{q} \cdot \xi_{ij}^\alpha = 0$ . So, only longitudinal modes participate in polar optical phonon scattering. Also, although not stated explicitly, the Frohlich interaction (78) vanishes in non-polar crystals. The reason for this is obvious on physical grounds—in a non-polar crystal, no dipole polarization can arise from optical mode displacements. Mathematically,

$$Z_1^\alpha = Z_2^\alpha, \quad \xi_{ij}^1 = -\xi_{ij}^2 \quad (79)$$

so the sum over  $\alpha$  vanishes.

The lowest order (in  $q$ ) long range acoustic mode process which doesn't vanish is the scattering due to quadrupole polarization. Piezoelectric scattering results from quadrupole polarization and can be present in both polar and non-polar crystals [25].

### 4.3.3 Phonon Scattering Rates

In the first part of this section the general electron-phonon matrix element, and the standard phenomenological electron-phonon matrix elements have been presented. To make use of these rates in a Monte Carlo simulation, we need to calculate from these matrix elements, the total scattering rates out of a particular state, and the differential scattering probability between a given final and initial state for use in the SCBE.

In section 2, it was stated that for weak perturbations and low electron energies, the Fermi Golden Rule (28) adequately described the scattering rate into a particular set of final states from a given initial state. The general form for the total scattering rate,  $S_{tot}(nk)$ , is the Golden Rule rate summed over all final states:

$$S_{tot}(nk) = \sum_{n'k'} \frac{2\pi}{\hbar} |\langle n'k' | V_p(r) | nk \rangle|^2 \delta(E_{n'}(k) - E_n(k) \mp \hbar\omega_q). \quad (80)$$

where  $\omega_q$  is the phonon associated with the particular scatterer in  $V_p(r)$ . This expression can be calculated exactly using the full electron-phonon matrix element in (53) as discussed in the chapter by Fischetti and Higman. However, it is standard practice for Monte Carlo simulations to take the much simpler route and calculate the scattering rates for the phenomenological matrix elements of the previous sections.

In fact, in order to obtain closed form expressions for these scattering rates, it is necessary to assume simple analytic forms for the band structure, the most general of which is the non-parabolic, ellipsoidal band structure describing the bands near the minimum of a "valley". The analytic form most often used is,

$$\gamma(E) = E(1 + \alpha E) = \frac{\hbar^2}{2} \left( \frac{(k_x - k_x^0)^2}{m_x} + \frac{(k_y - k_y^0)^2}{m_y} + \frac{(k_z - k_z^0)^2}{m_z} \right), \quad (81)$$

where  $k^0$  is the minimum of the valley. Accordingly, this description is only valid near the minimum of a particular valley. In general, the band structure is very complicated [33], and in the case of hot electron transport, the electrons are far these minima. One way to deal with this problem is to calculate the matrix elements discussed above for a full band structure. Another, much simpler way is to calculate the various scattering mechanisms valid near the minima and normalize the scattering rates to the density of states for higher energies [30]. This is a reasonable approach since most scattering rates are proportional to the density of states.

In this section the standard scattering rates valid near valley minima are discussed. Since the derivations leading to the scattering rates from the phenomenological matrix elements are well known and given in many texts (see for instance [34] and [36]), we quote only the results here. Typical values for the phenomenological parameters and material parameters for silicon are given in the appendix of this chapter.

However, as a preliminary, we list facts useful for deriving them. First,

to transform a summation over  $k'$  in (80) into a more manageable integral over  $k'$  we use the transformation [34]

$$\sum_{k'} \rightarrow \frac{V\alpha}{(2\pi)^3} \int dk' . \quad (82)$$

Note that spin is conserved in phonon collisions. Furthermore, if the  $m_i$  are equal, these integrals are normally done in spherical coordinates. Then the magnitude of  $k$  can be transformed into an integral over final energy  $E_f$  by use of the transformation,

$$dk' = dE_f \frac{(1 + 2\alpha E_f)m^*}{\hbar^3 k'} . \quad (83)$$

If the masses are unequal, the Herring-Vogt transformation is useful because it maps the problem into a "starred-space" which has a spherical  $E(k)$  relation [35]:

$$k_i^* \rightarrow k_i \sqrt{m_i} . \quad (84)$$

The problem is then solved in the "starred-space" and then transformed back to the physical space. As far as total scattering rates are concerned, this only has the effect of replacing  $m^*$  in the result by  $m_D \equiv (m_x m_y m_z)^{1/3}$ .

For intra-valley optical deformation potential scattering:

$$S_{i\alpha}(E) = \frac{D_{op}^2}{8\pi^2 \rho \omega_{op}} \left[ N_{\omega_{op}} + \frac{1}{2} \pm \frac{1}{2} \right] g(E \pm \hbar\omega_{op}) , \quad (85)$$

where  $g(E)$  is the density of states given by,

$$g(E) = \frac{(m_D)^{3/2}}{2^{1/2} \hbar^3 \pi^2} (1 + 2\alpha E)[E(1 + \alpha E)]^{1/2} , \quad E > 0 \quad (86)$$

and  $D_{op}$  is the optical deformation potential,  $\rho$  is the crystal density and  $\omega_{op}$  is the relevant optical phonon energy. To determine the final state after scattering, we only have to enforce energy conservation,  $E(k') = E(k) \pm \hbar\omega_{op}$ . Any state on this energy conserving surface is equally probable.

For inter-valley deformation potential scattering:

$$S_{i\alpha}(E) = \frac{D_{op}^2}{8\pi^2 \rho \omega_{iv}} Z_s \left[ N_{\omega_{iv}} + \frac{1}{2} \pm \frac{1}{2} \right] g(E \pm \hbar\omega_{iv} - \Delta_{iv}) , \quad (87)$$

where  $\omega_{iv}$  is the intervalley phonon energy for a particular phonon branch, and  $Z_s$  is the number of equivalent final valleys. For instance, in Silicon, there are six X-minima, and two "different" types of intervalley scattering. For scattering across to the X-minimum on the same axis (g-scattering),  $Z_s = 1$ ; for scattering to one of the minima on the plane perpendicular to the initial state axis (f-scattering),  $Z_s = 4$ .

$\Delta_{iv}$  is the energy difference between the initial and final state minima. For X-X scattering in silicon,  $\Delta_{iv} = 0$ . For  $\Gamma$ -L scattering in GaAs,  $\Delta_{iv} \approx 0.2\text{eV}$ . As in the intra-valley optical deformation potential scattering

$E \leq E_c$	Absorption	$x_{min} = 4E_c^{-1/2}(E_c^{1/2} - E^{1/2})/K_B T$ $x_{max} = 4E_c^{-1/2}(E_c^{1/2} + E^{1/2})/K_B T$
	Emission	None
$E \geq E_c$	Absorption	$x_{min} = 0$ $x_{max} = 4E_c^{-1/2}(E_c^{1/2} + E^{1/2})/K_B T$
	Emission	$x_{max} = 4E_c^{-1/2}(E_c^{1/2} - E^{1/2})/K_B T$ $x_{min} = 0$

rate,  $g(E)$  is the density of states in the final valley. The density of states plays an important role in all scattering rate determination, but it is most apparent in the expressions for the optical and intervalley deformation potential cases. The final state is selected randomly from all states conserving energy, and the final valley is picked randomly from the equivalent valleys. A list of typical intervalley phonons for Si is given in the appendix to this chapter.

**For intra-valley acoustic deformation potential scattering:** Because of the complicated tensor form for acoustic coupling, there is an intrinsic anisotropy in the coupling. However, as shown by Conwell, the effect of this anisotropy is small [24] and can be removed by a suitable averaging. This amounts to defining an average sound velocity  $v_s = (2v_t^2 + v_l^2)/3$  where  $v_t^2$  and  $v_l^2$  are the velocity of sound propagated by transverse and longitudinal modes respectively and an effective coupling strength  $\Xi$ .  $\Xi$  is usually chosen to fit experimental data. The acoustic phonon scattering rate is [36]:

$$S_{i\alpha} = \frac{\Xi^2(m_D)^{1/2}(K_B T)^2}{2^{5/2}\pi\rho\hbar^4 v_s^4} \gamma^{-1/2}(E) \int_{x_{min}}^{x_{max}} dx N^\pm(x) (1 + 2\alpha E \mp 2\alpha K_B T x) x^2 \quad (88)$$

with

$$N^\pm(x) = \left( \frac{1}{e^{\beta x} - 1} + \frac{1}{2} \pm \frac{1}{2} \right) \quad (89)$$

and the dimensionless limits of integration: where  $E_c \equiv \frac{1}{2}(m_D v_s^2)$ .

**For polar optical scattering:** The total scattering rate for polar optical phonon scattering has been calculated by Boardman-Fawcett-Swain which takes into account the overlap integrals in (78) [37]. These integrals can be evaluated for  $k$  and  $k'$  near the bottom of non-parabolic bands using  $k \cdot p$  perturbation theory. The result is:

$$I^2(k', k) = (a_b a_{b'} + c_b c_{b'} \cos \theta)^2 \quad (90)$$

$$a_b = [(1 + \alpha E(k))/(1 + 2\alpha E(k))]^{1/2}$$

$$c_b = [\alpha E(k)/(1 + 2\alpha E(k))]^{1/2}$$

(91)

where  $\theta$  is the angle between  $k$  and  $k'$ . Using this expression for the overlap integral, the total scattering rate for polar optical phonon scattering can be written:

$$S_{i\alpha}(E) = \frac{e^2 \omega_{LO} (m^*)^{1/2}}{2^{1/2} \pi \epsilon_0 \hbar} \frac{1 + 2\alpha E'}{\gamma(E)} \left( \frac{1}{\epsilon_\infty} - \frac{1}{\epsilon_0} \right) \left[ N_{\omega_{LO}} + \frac{1}{2} \pm \frac{1}{2} \right] \\ A \left( B \ln \left[ \frac{\gamma^{1/2}(E') + \gamma^{1/2}(E)}{\gamma^{1/2}(E') - \gamma^{1/2}(E)} \right] - C \right), \quad E \geq \hbar \omega_{LO} \quad (92)$$

where

$$A = [4(1 + \alpha E)(1 + \alpha E')(1 + 2\alpha E)(1 + 2\alpha E')]^{-1} \\ B = [2(1 + \alpha E)(1 + \alpha E') + \alpha(\gamma(E') + \gamma(E))]^2 \\ C = 2\alpha \gamma^{1/2}(E') \gamma^{1/2}(E) [4(1 + \alpha E)(1 + \alpha E') + \alpha(\gamma(E') + \gamma(E))] \\ E' = E - \hbar \omega_{LO}$$

Because of the  $1/q^2$  dependence of the matrix element and the angular dependence of the overlap integrals, polar optical phonon scattering is an anisotropic scattering mechanism. To choose the final state we can use the von Neumann rejection method to pick the angle  $\theta$  between  $k$  and  $k'$ , which is given by the probability density,

$$P(\theta) d\theta = \frac{(a_1 a_{1'} + c_1 c_{1'} \cos \theta)^2 \sin \theta d\theta}{\gamma(E') + \gamma(E) - 2\gamma^{1/2}(E') \gamma^{1/2}(E) \cos \theta}. \quad (93)$$

The azimuthal angle is completely random since the scattering probability density is independent of  $\phi$ . Thus, we can choose  $\phi$  with a uniform random number  $r$ :  $r \in [0, 1]$  by  $\phi = 2\pi r$ . The magnitude of the final state wavevector,  $k'$ , is selected by energy conservation for the given scattering event (phonon emission, or absorption), and thus, the final state vector is completely determined.

## 5 Impact Ionization

The multiplication of carriers by impact ionisation is of central importance in the theory of semiconductor devices both as a limiting mechanism and as a basis of device functionality. Impact ionisation is a two electron process, corresponding to the exact inverse of the Auger process: a highly energetic conduction band electron collides with a valence band electron which is ionised over the band gap, leaving two conduction electrons and a hole. The process can also occur for holes, in which a highly energetic hole creates two holes and an electron. Impact ionisation for holes can be seen as a "mirror image" of the impact ionisation for electrons, so we will treat only the electron impact ionisation.

As in section 1, the electron-electron interaction is designated as  $V_{ee}(r, r')$ , and following section 3, we screen the bare electron-electron interaction with the dielectric screening function. We will neglect the off-diagonal terms of

$\epsilon^{-1}(q + G, q + G'; \omega)$  and allow  $q$  to take on all values in the reciprocal lattice.

The bare electron-electron interaction is of course just the coulomb interaction between two electrons. Figure 2 shows the impact ionisation process schematically. States three and four are final conduction band electron states. State one is the initial electron state, and state two is the initial valence band electron state. The crystal momenta and band indices are designated as  $k_i$  and  $n_i$ , with  $i \in [1, 4]$ . Figure 2 shows the electron in states 1 and 2 interacting via the screened Coulomb potential to generate electrons in states 3 and 4. The final hole state corresponds to the missing valence electron in state two.

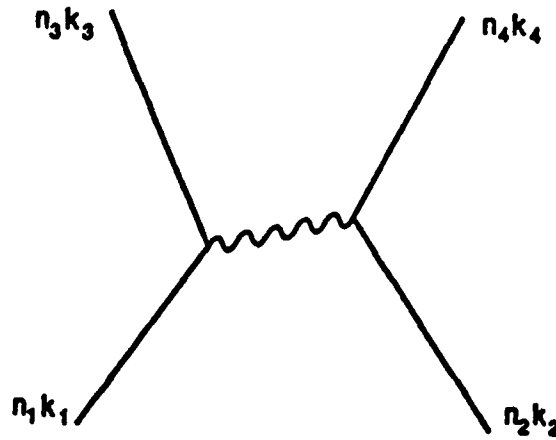


Figure 2: Schematic Representation of the screened electron-electron interaction corresponding to impact ionisation. Time is plotted vertically. Notice that the interaction is retarded due to dynamic screening effects.

Since  $V_{ee}(r, r')$  is a two particle interaction explicitly carrying two spatial coordinates, its matrix elements are between two-particle states. Since the electrons are fermions, the two-particle wave-functions must be anti-symmetric linear combinations of two-particle states with the Pauli spin matrices. We write these two-particle states as,

$$|n_1 k_1 \sigma_1; n_2 k_2 \sigma_2\rangle_A \equiv \frac{1}{\sqrt{2}} [\psi_{n_1, k_1}(r_1) \psi_{n_2, k_2}(r_2) \sigma_1(s_1) \sigma_2(s_2) - \psi_{n_1, k_1}(r_2) \psi_{n_2, k_2}(r_1) \sigma_1(s_2) \sigma_2(s_1)] \quad (94)$$

where the  $\sigma$  are the Pauli spin matrices, and  $s_1$  and  $s_2$  are the spin coordinates. The coordinate wave-functions  $\psi$  are normalized Bloch wave-functions. Also, we write the subscript  $A$  to signify the anti-symmetrised

state.

In this language, the event shown in figure 2 corresponds to the matrix element,

$$M(12; 34) \equiv \langle n_1 k_1 \sigma_1; n_2 k_2 \sigma_2 | {}_A V_{ee} | n_3 k_3 \sigma_3; n_4 k_4 \sigma_4 \rangle_A . \quad (95)$$

The matrix element contains four terms with different arrangements of the coordinates and the wavefunctions. For simplicity of notation we write the simple product states as  $| 12 \rangle = \psi_{n_1, k_1}(r_1) \psi_{n_2, k_2}(r_2)$ . Then, equation (95) expands as

$$M(12; 34) = \quad (96)$$

$$\frac{1}{2} [\delta_{\sigma_1, \sigma_3} \delta_{\sigma_2, \sigma_4} \langle 34 | V_{ee} | 12 \rangle - \delta_{\sigma_1, \sigma_4} \delta_{\sigma_2, \sigma_3} \langle 43 | V_{ee} | 12 \rangle - \delta_{\sigma_1, \sigma_4} \delta_{\sigma_2, \sigma_3} \langle 34 | V_{ee} | 21 \rangle + \delta_{\sigma_1, \sigma_3} \delta_{\sigma_2, \sigma_4} \langle 43 | V_{ee} | 21 \rangle] . \quad (97)$$

For a given initial state spin  $\sigma_1$ , there are three distinct physical situations, with equal probability of occurrence corresponding to the different configurations of the remaining spin indices. They are:

1.  $\sigma_1 = \sigma_2 = \sigma_3 = \sigma_4$
2.  $\sigma_1 \neq \sigma_2 : \sigma_1 = \sigma_3, \sigma_2 = \sigma_4$
3.  $\sigma_1 \neq \sigma_2 : \sigma_1 = \sigma_4, \sigma_2 = \sigma_3$

The rate for each configuration must be calculated separately, and then summed to give the total rate independent of spin. For instance, if we define,

$$\begin{aligned} M_1 &= \langle 34 | V_{ee} | 12 \rangle, \\ M_2 &= \langle 43 | V_{ee} | 12 \rangle, \end{aligned} \quad (98)$$

then the squares of matrix elements corresponding to the spin configurations in the list above (the probabilities) can be written in terms of  $M_1$  and  $M_2$  as:

1.  $| M_1 - M_2 |^2$
2.  $| M_1 |^2$
3.  $| M_2 |^2$ .

The sum of these probabilities gives the square of the total effective matrix element, summed over all internal spins for a given initial spin which we designate as  $M_{tot}^2$  and write as:

$$M_{tot}^2 = 2 | M_1 |^2 + 2 | M_2 |^2 - (M_1^* M_2 + M_2^* M_1). \quad (99)$$

Thus, we need only to calculate  $M_1$  and  $M_2$  to find the total rate. Furthermore, if we find an expression for  $M_1$ ,  $M_2$  is easily found by exchanging the final state indices, so we only calculate  $M_1$ .

The simplest way to include frequency dependent screening in calculating  $M_1$  above and the associated scattering rate  $S(12;34)$  is to calculate the two-particle propagator from  $|12\rangle$  to  $|34\rangle$  in time  $t$ , square it to obtain the probability, and take the time derivative for long times (time rate of change of the probability of going from  $|12\rangle$  to  $|34\rangle$ ):

$$S(12;34) = \lim_{t \rightarrow \infty} \frac{\partial}{\partial t} |\langle 34 | V_{ee} | 12 \rangle|^2 \quad (100)$$

This is wholly equivalent to the expression in section 2. In figure 2, the electron in state 1 feels the screened coulomb potential of state 2 at time  $t'$  and state 2 feels state 1 at time  $t''$ . The dielectric function retards the effects of states 1 and 2 on each other; for instance, even if electron 2 has passed electron 1, the valence electrons may still be readjusting to its passage and this can effect electron 1.

We write  $M_1 = \langle 34 | V_{ee} | 12 \rangle$  by letting states 1 and 2 propagate freely until times  $t'$  and  $t''$ , and then scatter into states 3 and 4 which propagate until time  $t$ . The potential felt at each time is weighted by  $\epsilon^{-1}(r'' - r'; t'' - t')$ . Then we must integrate over all  $t'$  and  $t''$ . This is basically a restatement of the Feynman rules for a first order, two-particle, time-dependent interaction which give

$$M_1 = \int d^3r \int d^3r' \psi_3^*(r) \psi_4^*(r') \psi_1(r) \psi_2(r') \sum_q \frac{e^2}{V \Omega q^2} e^{-iq \cdot (r-r')} I_q(t) \quad (101)$$

with

$$I_q(t) \equiv \int_0^t dt' e^{-i\omega_1 t'} e^{-i\omega_2 (t-t')} \int_0^{t'} dt'' e^{-i\omega_3 t''} e^{-i\omega_4 (t-t'')} \epsilon^{-1}(q, t' - t''). \quad (102)$$

In equation (101) we have written the Coulomb potential as a Fourier series over vectors in the reciprocal lattice  $q$ .  $I_q(t)$  is easily evaluated by making a change of variables in the  $t''$  integral to  $t' - t''$ . Then,

$$I_q(t) = e^{-i(\omega_1 + \omega_2)t} \int_0^t dt' e^{-i(\omega_1 + \omega_2 - \omega_3 - \omega_4)t'} \int_{t'-t}^{t'} dt'' e^{i(\omega_3 - \omega_4)t''} \epsilon^{-1}(q, t''). \quad (103)$$

Since we need only the large  $t$  limit, the inner integral becomes  $\epsilon^{-1}(q, \omega_3 - \omega_4)$ . In (101) we can evaluate the spatial coordinate integrals by using the trick in equation (56) section 4.

$$M_1 = \frac{1}{V \Omega} \sum_q \delta_{k_1, k_2 + q + G_1} \delta_{k_3, k_4 - q + G_2} \int_0 d^3r \int_0 d^3r' \frac{e^{i(k_1 - k_2 - q) \cdot r} e^{i(k_3 - k_4 + q) \cdot r'} u_3^*(r) u_4^*(r') u_1(r) u_2(r')}{q^2 \epsilon(q, \omega_3 - \omega_4)} I_q(t) \quad (104)$$

In the above equation,  $G_1$  and  $G_2$  are arbitrary reciprocal lattice vectors. For a given set of  $k_i$ ,  $q$  is determined up to a reciprocal lattice vector. We have the following crystal momentum conservation laws:

1.  $k_4 - k_3 + q + G_1 = 0$
2.  $k_3 - k_1 - q + G_2 = 0$
3.  $k_1 + k_2 - k_3 - k_4 = G_0 = G_1 + G_2$

The last equation, which follows from the first two, asserts the conservation of crystal momentum for the entire process. Furthermore, we can write each of the Bloch wavefunctions as sums over reciprocal lattice vectors (since they are lattice translation invariant):

$$u_{nh}(\mathbf{r}) = \sum_{\mathbf{G}} z_{nh}(\mathbf{G}) e^{i\mathbf{G}\cdot\mathbf{r}}. \quad (105)$$

Then,

$$M_1 = \delta_{k_1+k_2, k_3+k_4+G_0} \sum_{G_1, G_2, G_4} I_{k_1-k_2+G_1-G_2}(t) \quad (106)$$

$$\frac{z_1(\mathbf{G})z_2(\mathbf{G}_2 + \mathbf{G}_4 - \mathbf{G}_1 - \mathbf{G}_0)z_3^*(\mathbf{G}_2)z_4^*(\mathbf{G}_4)}{Vol |\mathbf{k}_1 - \mathbf{k}_2 + \mathbf{G}_1 - \mathbf{G}_2|^2} \quad (107)$$

This form is particularly well suited for numerical calculations since the expansions in (105) can be calculated by pseudopotential band structure calculations. To calculate the scattering rate given in (100), we must square (106) and take the time derivative. The only time dependence in the magnitude squared of  $I_q(t)$  is in the  $t'$  integral in equation (103). The time derivative of this gives the Golden rule rate expression as in equation (28).

Now, we can combine (106), (99) and (100) to obtain the total impact ionisation scattering rate  $S(12; 34)$  summed over secondary particle spins:

$$S(12; 34) = \frac{2\pi}{\hbar} |M_{tot}|^2 \delta(E_1 + E_2 - E_3 - E_4) \delta_{k_1+k_2, k_3+k_4+G_0}. \quad (108)$$

$$M_{tot} = |M_1|^2 + |M_2|^2 - \frac{1}{2}(M_1^* M_2 + M_2^* M_1)$$

$$M_i = \sum_{G_1, G_2, G_4} \frac{z_1(\mathbf{G})z_2(\mathbf{G}_2 + \mathbf{G}_4 - \mathbf{G}_1 - \mathbf{G}_0)z_3^*(\mathbf{G}_2)z_4^*(\mathbf{G}_4)}{Vol q_i^2 \epsilon(q, \omega_2 - \omega_4)}$$

$$q_1 = k_1 - k_2 + G_1 - G_2$$

$$q_2 = k_1 - k_4 + G_1 - G_4$$

$$G_0 = k_1 + k_2 - k_3 - k_4$$

This expression was first obtained by Kane [38].

To get the total scattering rate we need only sum over the two independent  $k$  vectors and the secondary particle band indices in  $S(12; 34)$ . Given  $n_1$  and  $k_1$ , the total impact ionisation scattering rate,  $S_{II}$ , from that

state is simply,

$$S_{ii}(n_1 k_1) = \sum_{n_2, n_3} \sum_{k_2, k_3} S(12; 34). \quad (109)$$

The wavevector sums (109) run over the first BZ.  $G_0$  is then the Umklapp wavevector necessary to ensure that  $k_2$  is in the first BZ for a given  $k_1$ .

To gain some qualitative insight into equation (109), we look at the two conservation laws it implies—conservation of crystal momentum and conservation of energy. First, energy conservation requires the initial electron to be at least  $E_g$  (gap energy) above the bottom of the conduction band in order to excite a valence electron across the gap and into some conduction band state. Therefore,  $E_g$  is a minimum energy for impact ionization. Additionally, the conservation of crystal momentum further shifts this minimum energy. The smallest energy necessary to initiate an impact ionization event in a particular band structure is known as the *impact ionization threshold energy*  $E_{ih}$ .

Some authors have defined a wavevector dependent  $E_{ih}$  by minimizing  $E_i$  (the initial electron energy) for a given  $k_i$  with the energy and momentum conservation constraints. This minimization procedure requires that [39]

$$\nabla_k E_2(k) = \nabla_k E_3(k) = \nabla_k E_4(k). \quad (110)$$

We shall re-evaluate the usefulness of this result later. Now we will look at the first attempt to evaluate the impact ionization scattering rate known as the Keldysh formula. The Keldysh formula makes two rather extreme approximations. The first is to approximate the matrix element as a constant, and the second, to assume simple parabolic bands. Of these, the second is very poor, yet the resulting formula, known as the Keldysh formula, has received considerable attention in the past. The result given by Keldysh involving the two adjustable parameters  $P$  and  $B$  is [40]:

$$S_{ii}(n_1 k_1) = \frac{B}{S_{ph}(E_{ih})} \left( \frac{E - E_{ih}}{E_{ih}} \right)^P. \quad (111)$$

Typically,  $1 \leq P \leq 2$  and  $S_{ph}$  is the total phonon scattering rate. Although this phenomenological form is simple to use, the approximations leading to it disregard the important features of the band structure, which at the high energies involved in impact ionization, has no resemblance to simple parabolic bands.

A much better solution for the impact ionization rate in silicon was given by E. O. Kane [38] in 1967. He numerically calculated the rate in equation (109) using the expressions developed in equation (108). First he calculated the pseudopotential band structure and wavefunctions (see the chapter by Fischetti and Higman) and used them to calculate the dielectric function in the RPA approximation (see equation (43)). The summations in equation (109) were evaluated by employing a Monte Carlo integration algorithm. The results of this calculation for  $S_{ii}(E)$ , ( $S_{ii}(k)$  averaged over all  $k$  with  $E(k) = E$ ) are shown in figure 3.

Figure 3 also plots the impact ionization scattering rate in silicon calcu-

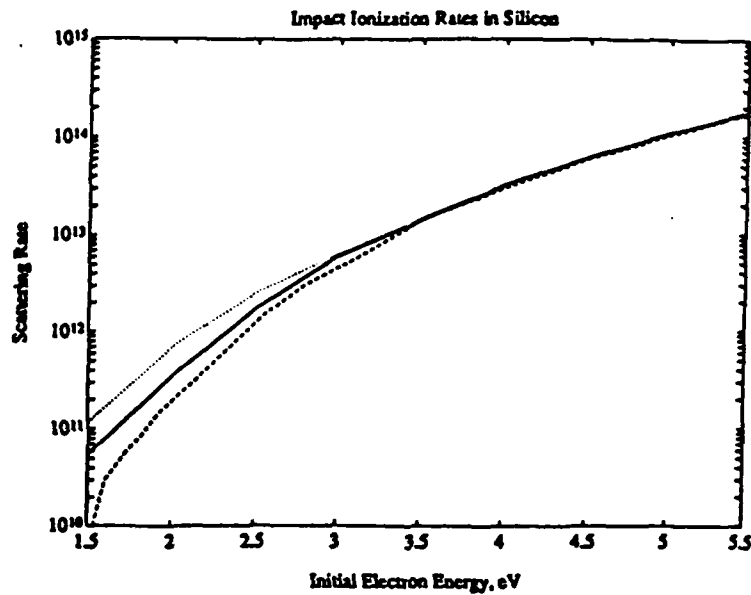


Figure 3: Impact ionisation rates in  $s^{-1}$  for silicon averaged over initial electron energy measured from the bottom of the conduction band. Dashed curve, Kane's result; solid curve, no collision broadening; dotted curve, collision broadening.

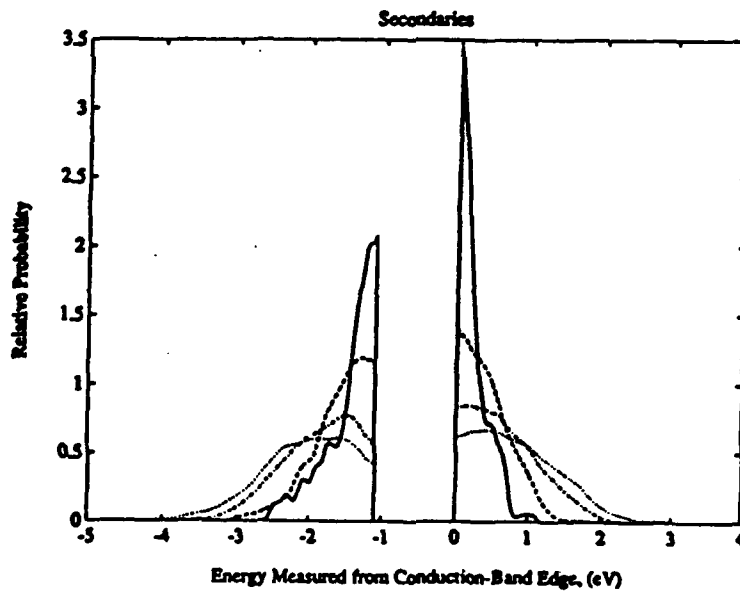


Figure 4: Secondaries produced by impact ionising electrons in silicon. Solid curve, initial electron of 1.5 eV; dashed curve, 2.5eV; dashed-dot, 3.5eV; dotted, 4.5 eV. The two sets of curves correspond to holes for the  $E < -E_G$ , and electrons, for  $E > 0$ .

lated to include the effects of collision broadening and the intra-collisional field effect (see section 2) [41]. The effects of high fields and high phonon scattering rates on the impact ionisation process shift the threshold down from that obtained by Kane. Figure 4 shows the distribution of secondaries (two final conduction electrons and a hole) produced initiating electrons of various energies. These distributions include collision broadening, which has a large effect near threshold.

Figure 5 addresses the question of  $k$ -space anisotropy for the impact ionization scattering rate. As discussed above, it is possible to calculate a wave-vector dependent threshold which would seem to be relevant to the anisotropy of the scattering rate. It is, however, difficult to guess an appropriate form for the scattering rate as a function of this threshold which is consistent with the true physics in equation (109). For instance, the wave-vector dependent scattering rate may not even be directly related to these thresholds for energies greater than  $E_{iA}(k)$ . Furthermore, if collision broadening is included (an important effect for high energy electrons for which the phonon scattering rate is high) the threshold condition is greatly relaxed. Figure 5 shows the impact ionization rate in silicon for electrons on the equi-energy surfaces  $E(k) = 2.5\text{eV}$  and  $E(k) = 3.0\text{eV}$  for electrons in the second conduction band in the  $k_x = 0$  plane [41]. As can be seen the scattering rate shows little anisotropy. In addition this energy range is important for impact ionization in transport calculations [42], so it is probably a good approximation to use the average, energy dependent scattering rates given in figure 3, for most Monte Carlo simulations.

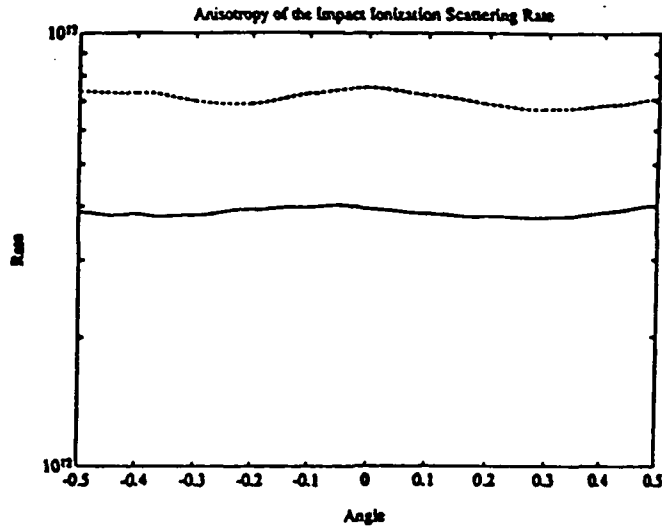


Figure 5:  $k$ -space anisotropy of the impact ionization scattering rate in silicon for electrons with  $k_x = 0$  on the equi-energy surfaces  $E = 2.5\text{eV}$  (solid line) and  $E = 3.0\text{eV}$  (dotted line). The angle is in units of  $\pi$  from the  $k_y$  axis.

## 6 Ionized Impurity Scattering

For even moderately doped semiconductors, ionized impurity scattering plays an important role and can dominate the total scattering rate for high doping concentrations. At 300K when doping densities reach levels above  $10^{17} \text{cm}^{-3}$ , scattering rates for ionized donors (acceptors) become comparable to low energy phonon scattering rates, while at low temperatures ionized impurity scattering becomes even more important since equilibrium phonon populations disappear exponentially as  $T \rightarrow 0$ . Thus, in cases of high doping or low temperatures, an accurate Monte Carlo model must include ionized impurity scattering.

Ionized impurities are usually assumed to be simple Coulomb potentials with a charge  $Ze$  ( $e$  the electron's charge). Typically they are associated with ionized acceptors or donors. At first glance one may propose that the ionized impurity perturbation  $V_i(r)$  is just this Coulomb potential, calculate the scattering rate for one impurity and multiply by the total number of impurities. Unfortunately, the calculation of ionized impurity scattering rates in this way is complicated by the long range nature of the Coulomb potential associated with the ions. Unscreened, the interaction of a single carrier and an ion leads to a diverging scattering rate which is of course an unphysical result. Therefore, the view of the ionized impurity interaction as one electron interacting with a single Coulombic potential cannot adequately describe the situation. Although there are many problems with this simplified model, the two most flagrant are the neglect of mobile charge screening, and the correlation of the other charges present. Each of these limits the effective length of the Coulomb interaction and removes the singularity. The first is treated by the Brooks-Herring Model [43], and the second by the Conwell-Weisskopf model [44]. A third model proposed by Ridley, called, *Third Body Exclusion*, reconciles these two approaches [45]. We will treat each in turn.

### 6.1 The Brooks-Herring Model

The Brooks-Herring model assumes that the electron (or hole) interacts solely with one ionized impurity site and deals with the many-body effects by introducing mobile charge screening. If mobile charge densities are high, it is necessary to include the effects of electronic screening, and these effects will limit the scattering rate to finite values.

Because the Brooks-Herring model assumes that a carrier sees each charge one at a time, in a semiconductor sample with  $N_D^+$  ionized donors and  $N_A^-$  ionized acceptors we must add the scattering rate due to each separately instead of using the net charge present. Thus, compensated ions can contribute to the total scattering rate as well. For this model, we will assume  $N_{tot}$  total ionized impurities of charge  $Ze$ .

Next we turn to Thomas-Fermi screening theory of section 3, equation (46). If the distribution function is Maxwellian, (46) reduces to the Debye-Huckel screening formula, introducing a screening length proportional to

the square root of the mobile carrier density  $n$ :

$$k_{TF}^2 = \frac{e^2 n}{\epsilon_0 \epsilon_r K_B T} \quad (112)$$

The Fourier transform of the screened ionised impurity potential  $V_i(q)$  is:

$$V_i(q) = \frac{Ze}{\epsilon_r \epsilon_0 q^2} \frac{1}{\epsilon_{TF}(q)} = \frac{Ze}{\epsilon_r \epsilon_0 (q^2 + k_{TF}^2)} \quad (113)$$

For  $K_{TF} \neq 0$  in equation (113) there is no divergence for small  $q$ , and therefore, there is no problem with infinite scattering rates. For degenerately doped semiconductors, the situation is more complicated, however an effective screening length can still be calculated from (46).

In real space, the Coulomb potential acquires an exponential tail as:

$$V_i(r) = \frac{Ze^2}{4\pi\epsilon_r\epsilon_0 |r-R|} e^{-k_{TF}|r-R|} \quad (114)$$

where  $R$  is the location of the ion. It should be emphasised that the screened potential approximation is not necessary to limit the cross section to finite values. In fact, at low mobile charge density,  $k_{TF}$  may not be sufficient to screen the potential and a model similar to the Conwell-Weisskopf method must be used.

In this section we will assume simple plane wave states for the electrons which is a good approximation for low energies. Ionized impurity scattering is essentially important only for low energy electrons, because, the phonon scattering rate dominates the impurity scattering rate for high electron energies.

We write the perturbation matrix element between plane wave states as  $M_{kk'}$ , where  $k$  is the incident wave vector and  $k'$  is the scattered wave vector as

$$M_{kk'} = \frac{1}{V} \int e^{-ik \cdot r} \frac{Ze^2}{4\pi\epsilon_r\epsilon_0 |r-R|} e^{-k_{TF}|r-R|} e^{ik' \cdot r} d^3r \quad (115)$$

( $V$ , the volume of the crystal, enters because of normalisation). The matrix element in equation (115) is found by taking the integral over into spherical coordinates with the azimuthal axis being in the direction of  $q \equiv k' - k$ . The result is:

$$M_{kk'} = \frac{iZe^2 e^{iR \cdot q}}{\epsilon_r \epsilon_0 q V} \frac{q}{k_{TF}^2 + q^2} \quad (116)$$

Finally, the scattering rate  $S(k, k')$  is given by the Fermi Golden Rule (see equation (28)). From equation (116) we can calculate the total scattering rate  $S_{tot}$  by integrating  $S(k, k')$  over all  $k'$ . Assuming spherical non-

parabolic bands,

$$S_{i\alpha} = \frac{2\pi (Ze^2)^2}{\hbar \epsilon_r^2 \epsilon_0^2 Vol^2} \frac{\hbar^2}{(1 + 2\alpha E_f)m^*} \frac{Vol}{8\pi^3} 2\pi \int_{-1}^1 du \int_0^\infty \frac{k' dE_f \delta(E_f - E_i)}{(k^2 + k'^2 - 2k'^2 u + k_{FP}^2)^2} \quad (117)$$

Here,  $u$  is the cosine of the angle between  $k$  and  $k'$ . Since the ion is strongly coupled to the lattice and is much more massive than the electron, the interaction can be treated as elastic, and we can take the term  $E_f$  equal to the energy of the final electronic state with wave vector  $k'$  and  $E_i$  equal to the energy of the initial electronic state with wave vector  $k$ .

The total scattering rate is [43]

$$S_{i\alpha} = \frac{N_I}{32\pi(2m^*)^{\frac{1}{2}}} \left( \frac{Ze^2}{\epsilon_r \epsilon_0} \right)^2 \frac{(1 + 2\alpha E)}{\gamma^{3/2}(E)} \left[ \frac{1}{(k_{FP}/2k)^2 (1 + (k_{FP}/2k)^2)} \right] \quad (118)$$

where  $N_I$  is the total density of impurities ( $N_I = N_{i\alpha}/Vol$ ). It is important to notice that we have simply summed the interaction of a plane wave and a Coulombic center over all the centers present; we have not calculated any many-body effect other than mobile charge screening—the calculation is a two-body calculation. The probability of a scattering into angular increment  $d\theta$  about  $\theta$ , ( $\theta$  is the angle between  $k$  and  $k'$ )  $P(\theta)d\theta$  is

$$P(\theta)d\theta = \frac{\sin \theta d\theta}{(2k^2(1 - \cos \theta) + k_{FP}^2)^2} \quad (119)$$

To relate  $P(\theta)d\theta$  to a uniformly chosen random number, we need only find the normalized probability that  $\theta$  lies between 0 and  $\theta$ . The result of this normalization allows us to determine  $\theta$ :

$$\cos \theta = 1 - \frac{2(1 - \tau)}{1 + 4\tau(k/k_{FP})^2} \quad (120)$$

Thus, we can stochastically determine the final state with only two random numbers, one for  $\phi$  and one for  $\theta$ .  $k'$  must equal  $k$  because the scattering is elastic and  $k$  is predetermined. If the bands are ellipsoidal, non-parabolic bands, we can use the Herring-Vogt transformation mentioned in section 4 equation (84). We need only make two modifications. First, we replace  $m^*$  by  $m_D$  in equation (118). To choose the final state we pick a  $k'$  using (120). Then, we transform it back from the Herring-Vogt space (see equation (84)).

It should however, be emphasized that the screened potential is not necessary to limit the scattering rate to finite values. In fact, for low mobile charge density,  $k_{FP}$  may not be sufficient to screen the potential and a model such as the Conwell-Weisskopf model may be more correct.

## 6.2 Conwell-Weisskopf Model

For comparison with the Brooks-Herring model, we compute the scattering cross section for the Conwell-Weisskopf model which assumes screening by other ions instead of screening by mobile charges. The Conwell-Weisskopf model assumes that the electron is fairly well localised instead of being an infinite plane wave as assumed in the Brooks-Herring model. This assumption remains useful up to moderate energies where the electron is considered a wave packet following a classically defined orbit. By localising the electron, we can see that in certain positions (midway between ions), the Coulomb forces from each tend to cancel and there is no interaction. In this spirit, Conwell and Weisskopf limit the impact parameter  $b$  to half of the mean distance between ions,

$$b_{\max} = \frac{1}{2} N_I^{-1/3} \quad (121)$$

where the impact parameter for classical Rutherford scattering is the closest approach of the electron to the ion if its path weren't deflected by the Coulombic force. Thus, this model effectively screens out the Coulomb force to the average distance between ions, and the unscreened Coulomb potential can be used to calculate the scattering rate classically with the Rutherford scattering model [44]. The scattering rate evaluated in this way is:

$$S_{\text{tot}}(k) = \frac{\pi v(k)}{4} N_I^{1/3} \quad (122)$$

where  $v(k)$  is the electron's velocity. The electron equation of motion states that  $v(k) = (1/\hbar)\nabla_k E(k)$ . For parabolic bands then,  $v(k) = (\hbar k)/m^*$ .

Not only is the Conwell-Weisskopf model more applicable for low doping densities than the Brooks-Herring model, but it also behaves more reasonably for high doping densities than the Brooks-Herring model. If we plot mobility versus  $N_I$  for both models, we see that the two agree very well for  $N_I < 10^{17} \text{ cm}^{-3}$ .

## 6.3 Third Body Exclusion

Both models presented above imply two-body, nearest-scatterer processes, but don't expressly prohibit scattering from more distant scattering centers. Ridley argues that, for the sake of consistency, the differential cross-section  $\sigma(k, \theta, \phi)$  must be weighted by the probability the scattering is a nearest-scatterer process. In doing so, he has found that the limiting cases of both the Brooks-Herring and the Conwell-Weisskopf models can be obtained. The method of weighting the cross-section in this manner is called third-body exclusion. (Note: the classical scattering cross-section is related to the scattering rate by  $S(k, \phi, \theta) = N_I v(k)\sigma(k, \theta, \phi)$ ).

In order to determine the appropriate factor we again employ the classical notion of the impact parameter  $b$ . Ridley has calculated the probability,  $P(b)$ , that no scattering center exists with impact parameter less than  $b$

from the probability  $p = 2\pi N_I a b db$  that such a center exists:

$$P(b) = e^{-\pi N_I a b^2} . \quad (123)$$

Here,  $a$  is the average distance between ions. Therefore, to prohibit third-body processes, the probability of a scattering event occurring in the solid angle  $d\Omega$ , must be multiplied by  $P(b)$ . Thus, we need only calculate  $b$  corresponding to the cross-section  $\sigma$  we wish to use. If we take  $\sigma$  from the Brooks-Herring model, we can obtain the limiting cases of both models, so we follow Ridley and calculate the corrected differential cross-section for it [45].

$\sigma_C$  the corrected cross-section, can be calculated easily from the Brooks-Herring cross-section  $\sigma_{BH}$  by the following:

$$\sigma_C = 2\pi \int_0^\pi \sigma_{BH}(k, \theta) e^{-\pi N_I a b^2} \sin \theta d\theta \quad (124)$$

Roer and Widdershoven give the scattering rate  $S_C = N_I v(k) \sigma_C$  as [46]

$$S_C = \frac{v(k)}{a} \left[ 1 - \exp\left(-\frac{a S_{BH}}{v(k)}\right) \right] \quad (125)$$

This scattering rate incorporates screening of both types (mobile and fixed charges) because it contains both  $k_{TF}$  and an ionic screening cutoff from the term in equation (123). Furthermore, it has the advantage that the total scattering rates are ten to a hundred times lower than the peak values of the Brooks-Herring and Conwell-Weisskopf models. This is quite important for Monte Carlo simulations because the higher the scattering rate for all mechanisms, the smaller the time step must be, forcing simulation runs to take much longer times. Roer and Widdershoven also show that at least in the case of GaAs, the low field impurity limited mobilities agree well with experimental results [46].

To find an expression for the angular distribution from the third-body exclusion model, we notice that the probability that an electron has an impact parameter  $b$  is  $pP(b) = 2\pi N_I a d e^{-\pi N_I a b^2} db$ . This is simply the product of the probability that a scattering center exists at a distance  $b$  and the probability that no other scattering center is closer. We can relate  $P(b)db$  to a uniform random number  $r : r \in [0, 1]$  by the relation:

$$r = \frac{\int_0^b b' e^{-\pi N_I a b'^2} db'}{\int_0^{b_{max}} b' e^{-\pi N_I a b'^2} db'} = \frac{e^{-\pi N_I a b^2} - 1}{e^{-\pi N_I a b_{max}^2} - 1} . \quad (126)$$

Since the relationship between  $r$  and  $b$  is transcendental, the Von-Neumann rejection method must be used to select a value of  $b$ . Then the scattering angle  $\theta$  can be determined from  $b$  by inverting the relation

$$\pi b^2(\theta) = \int_0^\pi \sigma_{BH}(k, \theta') \sin \theta' d\theta' \quad (127)$$

Then, the relation between  $\theta$  and  $b$  is

$$\cos \theta = 1 - \frac{1}{2k^2} \left[ \left( \frac{2k^2 \pi b^2}{K^2} + \frac{1}{4k^2 + k_{TF}^2} \right)^{-1} - k_{TF}^2 \right] \quad (128)$$

with

$$K^2 = \frac{(Ze^2)^2 (1 + 2\alpha E) m^* k}{4\pi \hbar^2 e^2 \epsilon_0^2 v(k)} \quad (129)$$

Although still a rather crude model, third-body exclusion is a compromise including screening of both types which limits scattering rates to manageable levels and fits experimentally obtained low field mobilities fairly well. At high fields, the Born approximation breaks down and other methods must be sought to include collision broadening effects.

## 7 Acknowledgement

This work has been supported by the Army Research Office, NSF through NCCE, and by the Office of Naval Research. The author would like to thank Jack Higman, Yoshitaka Tanimura, Chris Lee, and Doug Yoder for helpful and insightful conversations, and Karl Hess for his guidance.

## Appendix

### Table of Physical Constants and Phonon Scattering Parameters for Silicon

The following table gives typical parameter values and material constants for Si which occur in the formulas of section 4. Note that intervalley phonon energies are given in degrees Kelvin ( $\hbar\omega = k_B T_{\text{phonon}}$ ). Also, the models shown here are two-valley models- X and L valleys.

	Units	Tang [30]	Canali [47]	Sano [48]	Yoder [42]
$a$	Å	5.43		5.43	5.43
$\rho$	$\text{g/cm}^3$	2.329	2.329	2.329	2.329
$\epsilon$	$\epsilon_0$	11.7	11.7		
$v_s$	$10^8 \text{ cm/s}$	9.04	9.037	9.04	9.04
$m_{nt}$	$m_0$	0.19	0.1905	0.19	0.19
$m_{nl}$	$m_0$	0.9163	0.9163	0.916	0.916
$\alpha_e$	eV	0.5	0.5	0.5	0.5
$X_{ie}$	eV	9.5	9.0	9.0	9.5
$m_{H1}$	$m_0$	0.12		0.12	0.12068
$m_{H2}$	$m_0$	1.59		1.59	1.5942
X-X Intervalley Scattering					
$f_1$	$\text{K} (10^4 \text{ eV/cm})$	220 (0.3)	210 (0.15)	210 (0.15)	220 (0.3)
$f_2$		550 (2.0)	500 (3.4)	500 (3.4)	550 (1.9)
$f_3$		685 (2.0)	630 (4.0)	630 (4.0)	685 (1.9)
$g_1$		140 (0.5)	140 (0.5)	140 (0.5)	140 (0.5)
$g_2$		215 (0.8)	210 (0.8)	210 (0.8)	215 (1.1)
$g_3$		720 (11.0)	700 (3.0)	700 (3.0)	720 (4.3)
X-L Intervalley Scattering					
1	$\text{K} (10^4 \text{ eV/cm})$	672 (2.0)		672 (4.0)	672 (1.8)
2		634 (2.0)		634 (4.0)	634 (1.8)
3		480 (2.0)		480 (1.8)	480 (1.8)
4		197 (2.0)		197 (1.8)	197 (1.8)

## References

- [1] W. Jones and N. H. March, *Theoretical Solid State Physics*, pp. 611-613, Dover Publications, Inc., New York (1985).
- [2] P. Vogl "The Electron-Phonon Interaction in Semiconductors," pp. 75-116, in *Physics of Nonlinear Transport in Semiconductors* edited by D. K. Ferry, J. R. Barker and C. Jacoboni, Plenum Press, New York, (1979).
- [3] J. M. Ziman, *Elements of Advanced Quantum Theory*, pp. 1-12, Cambridge University Press, New York, (1988).
- [4] G. D. Mahan, *Many-Particle Physics*, p. 12, Plenum Press, New York, (1981).
- [5] R. Kubo, M. Toda, N. Hashitsume, in *Statistical Physics*, Springer-Verlag, New York, (1985).
- [6] A. L. Fetter, J. D. Walecka, in *Quantum Theory of Many Particle Systems*, McGraw-Hill Book Company, New York, (1971).
- [7] Y. C. Chang, D. Z. Y. Ting, J. Y. Tang, and K. Hess, *Appl. Phys. Lett.*, **42**, 1 (1983).
- [8] A. Messiah, *Quantum Mechanics*, John Wiley and Sons, New York, (1958).
- [9] J. R. Barker, *J. Phys. C: Solid State Physics*, **6**, pp. 2663-2684, (1973).
- [10] J. R. Barker, "Quantum Transport Theory," pp. 126-152, in *Physics of Nonlinear Transport in Semiconductors* edited by D. K. Ferry, J. R. Barker and C. Jacoboni, Plenum Press, New York, (1979).
- [11] D. K. Ferry, *Semiconductors*, Macmillan Publishing Company, New York, (1991). See especially the works of D. K. Ferry and J. R. Barker and of I. B. Levinson as well as the other references in chapter 15.
- [12] K. Kim, B. Mason, K. Hess, *Phys. Rev. B*, **36** No. 12, p. 6547 (1987).
- [13] L. Reggiani, *Physica Scripta*, **T23**, p. 218 (1988).
- [14] L. Sham and J. M. Ziman, "Solid State Physics - Advances in Research and Applications," pp. 270-274, in *Solid State Physics* edited by F. Seitz, D. Turnbull, and H. Ehrenreich, Academic Press, New York (1963).
- [15] N. W. Ashcroft, N. D. Mermin, *Solid State Physics*, pp. 338-340, Saunders College, Philadelphia, (1976).
- [16] H. Ehrenreich, M. H. Cohen, *Phys. Rev.*, **115**, p. 786, (1959).
- [17] G. D. Mahan, *Many-Particle Physics*, pp. 405-437, Plenum Press, New York, (1981).

- [18] N. W. Ashcroft, N. D. Mermin, *Solid State Physics*, pp. 422-450, Saunders College, Philadelphia, (1976).
- [19] J. M. Higman, "Rigid Pseudo-Ion Calculation of the Intervalley Electron-Phonon Interaction in Silicon," pp. 131-136, in *Computational Electronics*, edited by K. Hess, J. P. Leburton, U. Ravaioli, Kluwer Academic Publishers, Boston, (1991).
- [20] P. Bruesch, *Phonons: Theory and Experiments I*, p.63, Springer Verlag, New York, (1982).
- [21] W. Shockley, *Bell System Technical Journal* 30, 990, (1951).
- [22] W. Shockley and J. Bardeen, *Phys. Rev.*, 77 pp.407-408 (1950).
- [23] J. Bardeen and W. Shockley, *Phys. Rev.*, 80 p.72 (1950).
- [24] Conwell, E. M., "High Field Transport in Semiconductors," in *Solid State Physics*, edited by F. Seitz, D. Turnbull, and H. Ehrenreich, Supplement 9, Academic Press, New York, (1967).
- [25] B. K. Ridley, *Quantum Processes in Semiconductors*, pp. 106-130, Oxford Press, Oxford, (1988).
- [26] W. Harrison, *Phys. Rev. B*, 104, p. 1281, (1956).
- [27] G. L. Bir, G. E. Pikus, *Sov. Physics - Solid State*, 2, p. 2039, (1961).
- [28] D. Long, *Phys. Rev. B*, 120, No. 6, p. 2077 (1960).
- [29] Canali, *Phys. Rev. B*, 12, No. 4, p. 2275 (1975).
- [30] J. Y. Tang, "Theoretical Studies of High Energy Transport in GaAs, Si and Heterostructures," Ph. D. Thesis, University of Illinois, Champaign, Urbana, (1983).
- [31] M. V. Fischetti, *IEEE Trans. Electron Devices*, (1991). to appear
- [32] R. Evrard, "The Frohlich Polaron Concept," in *Polarons in Ionic Crystals and Polar Semiconductors*, pp. 37-4, edited by Josef T. Devreese, American Elsevier Publishing Company, New York (1972).
- [33] Cohen, M. L., and T. K. Bergstresser, *Phys. Rev.*, 141, p. 789, (1966).
- [34] K. Hess, *Advanced Theory of Semiconductor Devices*, Prentice Hall, Englewood Cliffs, New Jersey, (1988).
- [35] C. Herring and E. Vogt, *Phys. Rev.*, 101, p. 994, (1956).
- [36] C. Jaoboni, L. Regianni, "The Monte Carlo Method for the Solution of Charge Transport in Semiconductors with Application to Covalent Materials," *Review of Modern Physics* 55, No. 3 p. 645, (1983).
- [37] W. Boardman, A. D. Fawcett, S. Swain, *J. Phys. Chem. of Solids*, 31, p. 1963, (1970).

- [38] E. O. Kane, *Phys. Rev.*, **159**, p. 624, (1967).
- [39] C. L. Anderson and C.R. Crowell *Phys. Rev. B*, **5**, p. 2267, (1972).
- [40] L. V. Keldysh, *Sov. Phys. JETP*, **21**, p. 1135 (1965).
- [41] J. Bude, K. Hess, G. J. Iafrate, "Impact Ionization in Semiconductors: Beyond the Golden Rule," to be published.
- [42] D. Yoder, MS Thesis, University of Illinois, May 1991.
- [43] H. Brooks, C. Herring, *Phys. Rev.*, **83**, p. 879, (1951).
- [44] E. Conwell, V. F. Weisskopf, *Phys. Rev.*, **77**, No. 3, pp. 388-390, (1950).
- [45] B. K. Ridley, *J. of Phys. Chem.*, **bf 10**, pp. 1589-1593, (1977).
- [46] T. G. Van de Roer, and F. P. Widdershoven, *J. of Appl. Phys.*, **59**, No. 3, pp. 813-815, (1986).
- [47] C. Canali, C. Jaoboni, F. Nava, G. Ottaviani, and A. Alverigi-Quaranta, *Phys. Rev. B*, **12**, pp. 2265-2284, (1974).
- [48] N. Sano, T. Aoki, M. Tomizawa, A. Yoshii, *Phys. Rev. B*, **41**, pp. 12122-12128, (1990).